Quaternary Science Reviews 202 (2018) 166–181

Contents lists available at ScienceDirect

Quaternary Science Reviews

journal homepage: www.elsevier.com/locate/quascirev

Late Quaternary climate change in the north-eastern highlands of Ethiopia: A high resolution 15,600 year diatom and pigment record from Lake Hayk

Katie L. Loakes [a, *], David B. Ryves [a], Henry F. Lamb [b], Frank Schäbitz [c], Michael Dee [d], Jonathan J. Tyler [e], Keely Mills [f], Suzanne McGowan [g]

[a] Department of Geography, Loughborough University, Loughborough, Leicestershire, LE11 3TU, UK
[b] Department of Geography, Aberystwyth University, Aberystwyth, SY23 3DB, UK
[c] University of Cologne, Institute of Geography Education, Gronewaldstr, Köln, 2D-50931, Germany
[d] Research Laboratory for Archaeology and the History of Art, Dyson Perrins Building, South Parks Rd, Oxford, OX1 3QY, UK
[e] Department of Earth Sciences and Sprigg Geobiology Centres, The University of Adelaide, Adelaide, 5005, South Australia, Australia
[f] British Geological Survey, Keyworth, Nottingham, NG12 5GG, UK
[g] School of Geography, University of Nottingham, University Park, Nottingham, NG7 2RD, UK

ARTICLE INFO

Article history:
Received 16 February 2018
Received in revised form
26 July 2018
Accepted 4 September 2018
Available online 16 October 2018

Keywords:
African Humid Period
Ethiopia
Lake level
Diatoms
Pigments
Heinrich event
Holocene
Palaeolimnology

ABSTRACT

Multi-proxy analyses of an 8 m sediment core from Lake Hayk, a closed, freshwater lake in the north-central highlands of Ethiopia, provide a record of changing lake level and inferred regional climatic change for the last 15.6 cal ka years. Between ca. 15.6–15.2 cal ka BP, a lowstand was synchronous with Heinrich Event 1 and an intense drought across Eastern Africa. At ca. 15.2 cal ka BP a lake began to develop at the core site in response to wetter conditions, at the onset of the African Humid Period (AHP). However, in contrast to other lakes in eastern Africa, Hayk lake level fell around ca. 14.8 cal ka BP, indicating a climate shift towards aridity. The lake began filling again at ca. 12.3 cal ka BP and reached maximum water depth between ca. 12.0–10.0 cal ka BP. Lake level declined slowly during the Holocene, culminating in the termination of the AHP at Hayk between ca. 5.2–4.6 cal ka BP. In the late Holocene, ca. 2.2–1.3 cal ka BP, Lake Hayk was again deep and fresh with some evidence of short-term lake level variability.

The palaeo-record from Lake Hayk indicates that while it experienced, to a broad degree, the same glacial-interglacial dynamics and sub-millennial shifts in climate found in other palaeolimnological records from eastern Africa, there are offsets in timing and rate of response. These differences reflect chronological discrepancies between records, as well as the varying climate sensitivities and site-specific factors of individual lake basins. This record highlights the different responses by lakes in a climatically vulnerable area of Ethiopia.

1. Introduction

Northern Ethiopia is a climatically sensitive region due to its location close to the northernmost limit of the Inter Tropical Convergence Zone (ITCZ). Even slight displacement in position or change in strength of the monsoon system can cause switches between aridity and moisture surplus. Sedimentary records from Lakes Ashenge (Marshall et al., 2009) and Tana (Lamb et al., 2007a; Marshall et al., 2011; Costa et al., 2014) indicate that the region is strongly influenced by millennial-scale variations in the monsoon system. However, local site-specific mechanisms may have affected the expression of climate change during the late Quaternary.

Lake Hayk (also spelled Hayq and Haik), close to Lake Ashenge, provides a test of the extent to which site-specific effects influence the sedimentary record of climatic events. Here a multi-proxy sedimentary record from Lake Hayk is presented, focussing on diatom and photosynthetic pigment analyses. We examined the lake's palaeolimnological archive in order to determine the nature and timing of millennial-scale hydrological changes during the late

* Corresponding author.
E-mail addresses: katiell03@aol.com (K.L. Loakes), D.B.Ryves@lboro.ac.uk (D.B. Ryves).

https://doi.org/10.1016/j.quascirev.2018.09.005
0277-3791/

Quaternary. These include Heinrich Event 1 (ca. 17.0–16.0 ka BP), the Younger Dryas Stadial (ca. 12.8–11.6 ka BP), the African Humid Period, and more contested episodes such as drought events at ca. 8.2 ka BP and ca. 4.2 ka BP. There is no clear consensus on the abruptness of these events and uncertainty remains regarding the timing and expression of these high-magnitude transitional periods based on the diverging response of biotic and hydrological systems. Differences are found not only between sites, but also within the same lake; palaeo-shorelines and hydrological modelling at Lake Suguta provide contrasting evidence of both a gradual and abrupt termination of the AHP (Junginger et al., 2013).

This gap in our understanding is amplified further by the uneven spatial representation of high-resolution palaeo-records from Ethiopia. Attention has only recently focused on records from the north (Lamb et al., 2007a, 2007b; Marshall et al., 2009, 2011) rather than the south, Main Ethiopian Rift or mountain regions. Therefore, understanding of the timing, expression and mechanisms of these climatic transitions in northern Ethiopia remains limited. This paleao-record sheds light on the spatial and temporal expression of regional drivers of climatic and hydrological change at a site affected by both the African and Indian Monsoon systems.

2. Regional setting

The Ethiopian climate is characterised by strong rainfall seasonality caused by the annual migration of the ITCZ. This gives rise to three seasons: intense rainfall from June to September (*kiremt*), dry conditions from October to January (*bega*) and lesser rains from February to May (the *belg*) (Umer et al., 2004). When superimposed over the large changes in elevation over short distances, a patchwork of seasonal rainfall patterns and microclimates can be identified across Ethiopia. Climate data from four weather stations within 50 km of the lake record total annual rainfall as 1000–1100 mm yr^{-1} with most rainfall (~79%) falling between April and September (Darbyshire et al., 2003). The mean annual temperature is 18°C with a diurnal range of 8–23°C.

Lake Hayk (11°20′53″N, 39°42′32″E; 1920 m altitude) lies on the eastern margin of the north-central highlands in the South Wollo province of the Amhara region, northern Ethiopia (Fig. 1). The lake lies in a graben in Tertiary volcanic bedrock. It has a surface area of 23.2 km^2, and a catchment area of 65.0 km^2. It is a deeply shelving lake with a mean depth of 37.4 m. In 1938 the maximum lake depth was 88.8 m but this had decreased to 81.0 m by 2000 (Lamb et al., 2007b). The main input to the lake is the Ankwarka River but there is no surface outlet. An apparent palaeochannel indicates that the nearby Lake Hardibo previously overflowed into Lake Hayk. The palaeochannel is now permanently dry and would require a 16–18 m rise in water level at Lake Hardibo to cause overflow again (Ghinassi et al., 2012). Occasional water flow now occurs between the lakes through an artificial irrigation canal. A second palaeochannel indicates that Lake Hayk overflowed during highstands into the Wazi River, a tributary of the Mille River which ultimately joins the Awash River in the south of the Afar Depression. It is estimated that a rise of approximately 40 m would be required to make Lake Hayk overflow again (Lamb et al., 2007b). Lake level changes in the 1970s and 1980s demonstrate the lake's hydrological sensitivity to inter-annual climate change and to human impact, largely through catchment land use (Yesuf et al., 2013).

Lake Hayk is fresh, with a conductivity of 920 μS cm^{-1} (Williams, 1967; Gasse, 1986) and pH 9 as recorded in 1969 (Baxter and Golobitsch, 1970). The water balance of the lake is relatively well understood given the availability of hydrometeorological data, field hydrogeological investigations and groundwater modelling (Demelie et al., 2007). Total annual inflow from precipitation, catchment runoff and rivers into Lake Hayk is 45.2 million m^3. Evaporation is the main water loss from the lake (65%), which combined with abstraction for irrigation, makes an annual loss of 34.6×10^6 m^3. Groundwater flows play a significant role in the lake's hydrology, with inflow (5.9×10^6 m^3 yr^{-1}, 11%) about a third of outflow (1.4×10^6 m^3 yr^{-1}, 3%) (Lamb et al., 2007b). Oxygen isotope composition of the lake water ranged from +7.1 to +9.1‰ between 1975 and 2001, indicating evaporative enrichment relative to the mean annual precipitation value of −1.2‰ and confirming the role of evaporation as a major influence on lake hydrology (Lamb et al., 2007b).

3. Materials and methods

3.1. Field sampling

Core Hayk-01-2010 (hereafter Hayk-10) was recovered from Lake Hayk in January 2010, using a UWITEC hammered piston corer, with a 5.8 cm diameter and 210 cm barrel. It was operated from a raft anchored in the lakes' northern basin at 78.2 m water depth (Fig. 1). Beginning 89 cm below the sediment surface, ca. 1200 cm was recovered as nine drives (hence the upper section was not sampled in 2010, rather than representing a sedimentary hiatus; see Lamb et al., 2007b). The cores were stored under refrigeration at Aberystwyth University in the original plastic core liners until split longitudinally for analysis in 2013.

3.2. Sedimentology

The Troels-Smith sediment classification scheme was applied to characterise and define the lithostratigraphic units of core Hayk-10 (Schnurrenberger et al., 2003). Organic (C_{org}) and carbonate content (CO_3^{2-}) was estimated at approximately 2 cm intervals using loss-on-ignition (LOI) at 550°C and 925°C, following standard methodology (Dean, 1974). Loss-on-ignition data served as the primary tool for identifying any depth discrepancies and overlap between cores, in conjunction with chronological and diatom data; based on overlapping sections, the composite core Hayk-10 was deemed to be 822 cm in length.

3.3. Radiocarbon chronology

In the absence of macrofossils and sufficient charcoal, fourteen bulk organic matter samples were extracted for AMS ^{14}C dating. Samples were treated following standard techniques; nine were sent to the 14CHRONO Centres' radiocarbon dating laboratory at Queens University Belfast and five to the Oxford Radiocarbon Accelerator Unit at the University of Oxford. Radiocarbon ages were corrected for isotope fractionation using the $\delta^{13}C$ measured by AMS. Results are reported as conventional radiocarbon years before present (yr BP) relative to AD 1950 and calibrated using CALIB Rev 7.0.2 (Stuiver and Reimer, 1993). The median probability of age is based on weighted average, two sigma probability distributions. An age-depth model was constructed based on a 0.4 span smooth spline interpolation using the programme CLAM (Blaauw, 2010).

3.4. Diatom analysis and conductivity reconstructions

Diatom preparation and analyses followed a standard methodology with counts at non-contiguous 0.5–2.0 cm intervals. Samples were mounted in Naphrax and counted under oil-immersion phase-contrast light microscope at x 1000 magnification using a Leica DMRA research microscope. At least 300 valves were counted per sample, except where diatom abundance was especially low. Percentage data are reported for all counts >50 valves. Taxonomy follows Krammer and Lange-Bertalot (1988, 1991; 1999), Gasse

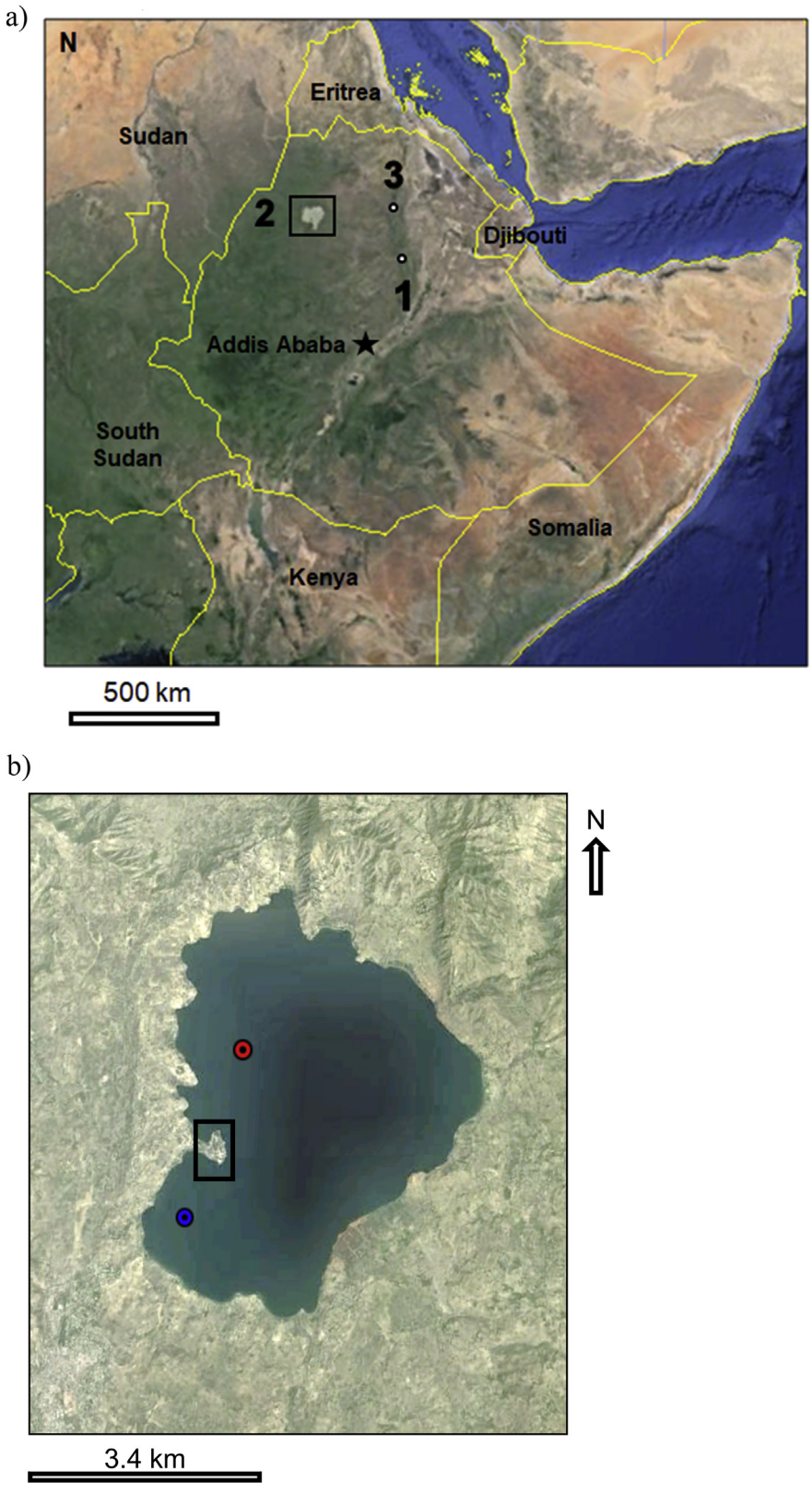

Fig. 1. (a) Location of Lake Hayk (1) on the eastern margin of the north-central highlands in northern Ethiopia. Lakes Tana (2) and Ashenge (3) are also indicated. (b) Aerial view of Lake Hayk. The red circle shows the location of core Hayk-01-2010. The blue circle indicates the approximate location of core HYK99-1 extracted in 1999 by Lamb et al. (2007b) and Darbyshire et al. (2003). The black box indicates the position of the Istifanos monastery, located on an island in the 9th century, which has since become attached to the mainland (Google Earth 2018). (For interpretation of the references to colour in this figure legend, the reader is referred to the Web version of this article.)

(1986), Hustedt (1949) and Patrick and Reimer (1966), with reference also made to other regional flora such as Cocquyt et al. (1993) and Cocquyt (1998). Diatom concentration was estimated by adding a known number of microspheres to the samples.

Assemblage zones were determined using the optimal sum of squares portioning method in the package PsimPoll 4.27 (Bennett, 1995–2007). Statistically significant splits were identified using a broken-stick model (Bennett, 1996). Ordination of diatom data was carried out using PCA on Hellinger-transformed data within Canoco 4.54.

Diatom data were used to make palaeosalinity inferences using the EDDI (European Diatom Database at http://craticula.ncl.ac.uk/Eddi/jsp/index.jsp) combined African dataset. Additionally, selected European sites from the EDDI database were added to the African training set to provide analogues for the earlier part of the Hayk sequence, most significantly for the species *Cyclotella ocellata*. This planktonic freshwater diatom was common (40–100%) in one section of the core (diatom zone Hayk-1b; 748-716 cm), but is poorly represented in the EDDI African training set (maximum abundance 8.5%), where its distribution is skewed to more saline sites, although unequivocally known to be freshwater. Its presence in other Ethiopian and African records has also resulted in problems with palaeosalinity inferences using the EDDI dataset (Chalié and Gasse, 2002a; Marshall et al., 2009). Analogue matching was used to find sites most similar among the European EDDI dataset, and these were carefully inspected before adding to the African salinity training set. The frequency distribution of *C. ocellata* against conductivity in this hybrid training set was further examined and several African sites removed that skewed this towards higher values (the model was also tested on another model with only sites added and the differences in performance and inference were negligible; see Loakes, 2015 for further detail). Twelve European sites were added to the model with up to 68.4% *C. ocellata*. Transfer function development was carried out in C2 v.1.7.2 (Juggins, 2007). The new training set comprised 251 sites and 852 species. Weighted averaging (WA) was used to produce the final model, as WA-PLS did not improve the performance assessed against RMSEP, with WA with inverse deshrinking performing best ($r^2 = 0.843$; RMSEP = 0.466 log units).

A simplified lake level curve, representing maximum depth at a relatively coarse temporal resolution, was based on comparison of modern conductivity (measured in 1969) and lake level (920 µS cm^{-1}, 81 m), and inferences from the sedimentology, and fossil diatom and pigment assemblages. For example, modern analogues of European lakes where *Cyclotella ocellata* (found towards the base of the Hayk sequence) is important, imply a maximum lake depth < 20 m (EDDI database). Similarly, the presence of green sulphur bacterial pigments (e.g. isorenieratene), and sections of finely laminated sediments, imply a water column deep enough for long-term anoxic stratification (meromixis). Together with knowledge of the autecology of other key diatom taxa (*Aulacoseira*, *Stephanodiscus*, long and slender *Fragilaria*, *Ulnaria* and benthic/epiphytic diatoms), we inferred the most likely maximum depth for core sections using this combined suit of multiproxy data.

3.5. Photosynthetic pigment analysis

Sedimentary pigments from freeze-dried samples at non-contiguous 0.5–14.0 cm intervals and weighing approximately 200 mg, were extracted following standard methodology. High performance liquid chromatography (HPLC) analysis was conducted using a modification of the method of Chen et al. (2001) on an Agilent 1200 Series separation module with Quaternary pump, autosampler, ODS Hypersil column (205 × 4.6 mm; 5 µm particle size) and the mobile phase of three solvents: solvent A (80: 20, methanol: 0.5 M ammonium acetate), solvent B (9: 1, acetonitrile: water) and solvent C (ethyl acetate). Pigments were identified and quantified by comparing retention times and the absorbance spectra of chromatogram peaks with an authentic standard under the same separation conditions (Roy et al., 2011). As commercial standards were unavailable for bacteriochlorophyll *e* (bchl *e*), isorenieratene and chlorobactene, they were identified based on their relative chromatogram positions and their concentrations were estimated by using calibration constants for chlorophyll *a* (for bacteriochlorophyll *e*) and for lutein (isorenieratene, chlorobactene). Assemblage zones were determined using the sample method as applied to the diatom stratigraphy, after being normalised using a log (x + 1) transformation.

4. Results and limnological interpretation

4.1. Chronology and lithology

The age-depth model shown in Fig. 2 is based on 14 AMS ^{14}C dates (Table 1). Hayk-10 covers the period from 15,600–1350 cal yr BP (the period 1350 cal yr BP to present was not retrieved during coring). Sedimentation rates vary over five main periods: (1) 15,600–15,450 cal yr BP (822.0–789.0 cm) sediment accumulation rate is relatively stable and high, averaging 0.2 cm yr^{-1}; (2) 15,450–12,200 cal yr BP (789.0–541.0 cm) sedimentation decreases to 0.05 cm yr^{-1} before increasing; (3) 12,200–11,800 cal yr BP (541.0–474.0 cm) accumulation is stable averaging 0.2 cm yr^{-1}; (4) 11,800 cal yr BP, sedimentation declines to 0.01 cm yr^{-1} (296.25 cm) before increasing; (5) 2500–1350 cal yr BP (200.0–89.5 cm) sedimentation averages 0.1 cm yr^{-1}. These rates are generally comparable to average sedimentation across the larger East African Rift Lakes, such as Lakes Malawi and Tanganyika, during the Holocene (0.1 cm yr^{-1}; Johnson, 1996).

Three lithostratigraphic units are defined in core Hayk-10 based on variations in composition and physical properties of the sediment layers (Fig. 3). The basal, and smallest unit (L-I, 822-797 cm)

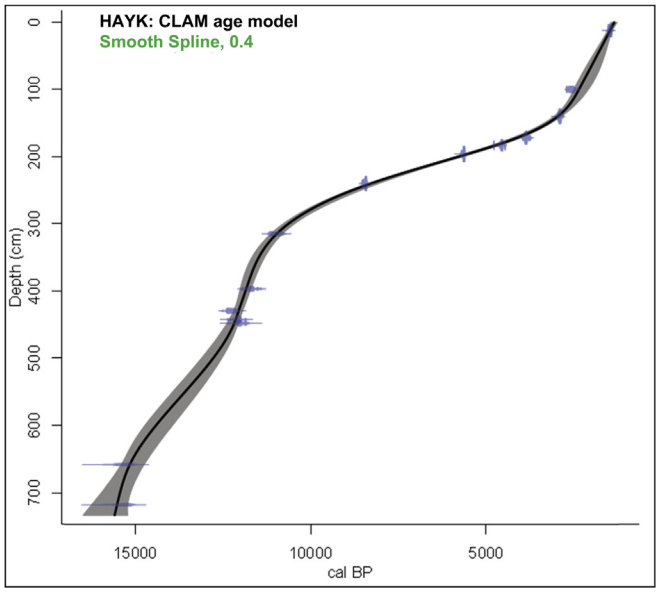

Fig. 2. Age-depth model of fourteen bulk AMS ^{14}C dates using CLAM. Depth refers to depth below the top of the sediment core. The individual age distribution for each date, as relative area under probability distribution, is shown in blue. The black line indicates the most likely age-depth distribution, whilst the grey envelope represents the model's chronological uncertainty. (For interpretation of the references to colour in this figure legend, the reader is referred to the Web version of this article.)

Table 1
AMS radiocarbon chronology of Lake Hayk, core Hayk-01-2010.

Laboratory	Laboratory reference	Depth below top of sediment sequence (cm)	Conventional age, ^{14}C yrs BP	Calibrated age, cal yr BP, weighted average, 2 sigma calibration (relative area under probability distribution)	Calibrated age, cal yr BP, median probability (to nearest 10 yrs)
^{14}CHRONO Centre	UBA-27072	12.5	1583 ± 32	1404 - 1545 (1.00)	1470
ORAU	OxA-30960	100	2485 ± 32	2432 - 2728 (0.99)	2580
ORAU	OxA-30883	140	2795 ± 31	2837 - 2965 (0.93)	2900
^{14}CHRONO Centre	UBA-25092	172	3563 ± 36	3816 - 3934 (0.74)	3860
ORAU	OxA-30885	183	4068 ± 33	4496 - 4645 (0.68)	4560
ORAU	OxA-30886	196	4914 ± 35	5592 - 5715 (1.00)	5640
ORAU	OxA-30887	240	7650 ± 45	8386 - 8540 (1.00)	8440
^{14}CHRONO Centre	UBA-27073	314.5	9643 ± 79	10749 - 11204 (1.00)	10970
^{14}CHRONO Centre	UBA-27074	396.5	10102 ± 44	11587 - 11840 (0.69)	11710
^{14}CHRONO Centre	UBA-25093	429	10393 ± 45	12061 - 12423 (0.98)	12270
^{14}CHRONO Centre	UBA-25094	442	10287 ± 46	11926 - 12241 (0.85)	12060
^{14}CHRONO Centre	UBA-27075	447.5	10254 ± 62	11756 - 12239 (0.96)	12000
^{14}CHRONO Centre	UBA-27076	657.5	12846 ± 67	15120 - 15596 (1.00)	15320
^{14}CHRONO Centre	UBA-25095	717.5	12873 ± 60	15157 - 15614 (1.00)	15360

consists of stiff black clay, intermixed with fine sand. Organic matter (6.5–7.1%), carbonate (4.8–6.5%) and water content (36.2–38.3%) are low in this unit. Accumulation rates for dry mass, organic and minerogenic matter are at maximum values. The overlying unit (L-II, 797-595 cm) is composed of grey gyttja intermixed with silt. Between 739.0 and 754.5 cm faint marl laminations are identifiable at irregular intervals. Organic matter remains low (4.7–10.8%). Carbonate content varies substantially (3.0–44.7%), whilst water content increases (37.6–75.8%). Dry mass, organic matter and minerogenic accumulation rates all plateau in this unit, whereas calcium carbonate accumulation is higher in the mid-zone (750–710.5 cm). The largest unit (L-III, 595-89 cm) consists of brown gyttja intermixed with silt. Traces of plant material are found in the top 70 cm. The unit contains irregularly spaced, thick (>1–7 mm) laminations consisting of a yellow, pulp-like material alternating with darker organics (Fig. 3). Smear slides of this yellow material show that it contains dense mats of the long, slender diatom taxa *Fragilaria* and *Ulnaria*. Organic matter reaches maximum values between 340 and 298 cm (38.0–30.7%) after which it declines. Water content is highest in this unit (74.8%). Dry mass, organic matter, minerogenic and calcium carbonate accumulation rates plateau in the mid-zone before increasing between 196 and 89 cm. The top 89 cm of sediment were not available for analysis.

4.2. Diatom and pigment data

The Hayk-10 sediment sequence is divided into nine diatom assemblage zones with taxa categorised and interpreted by habitat (Fig. 4). A summary diagram is presented in Fig. 5.

4.2.1. Hayk-1a (822-748 cm, 15,600–15,200 cal yr BP)

In this zone Lake Hayk was at a lowstand, expressed by negligible concentrations of diatoms and traces of benthic and aerophilous taxa. The presence of *Hantzschia amphioxys* provides evidence of a shallow lake environment and indicates sediment reworking from marginal or exposed areas in the catchment. This is in agreement with the compacted nature of the sediment as well as the low water content, which suggests the core site may have been exposed at times, possibly alternating between longer periods of dry, saline conditions and short wet episodes, when runoff in the catchment would have been channelled down the steep-sided lake basin to the core site. Diatom-inferred conductivity (800–9000 μS cm^{-1}) and variable preservation indicate the core site was slightly oligosaline to mesosaline, which may have prevented vegetation and soils from developing (Hammer, 1986). It was most likely an ephemeral lake, which dried out repeatedly during this time.

Pigment accumulation rate was similarly low during this period (<450 pmol cm^{-2} yr^{-1}), indicating poor preservation conditions. Over exposure to light, oxygen rich and high temperature conditions in a very shallow lake habitat, as well as physical reworking of the sediments and occasional drying out may have degraded pigments in the water column and in the uppermost sediments, preventing them from being incorporated into the fossil record.

4.2.2. Hayk-1b (748-716 cm, 15,200–14,800 cal yr BP)

The diatom record is dominated by *Cyclotella ocellata* (42–100%) during Hayk-1b, indicating an increase in lake depth and a degree of water permanence, caused by wetter conditions. The taxon has a wide ecological tolerance in terms of trophic state, being present in ultra-oligotrophic to eutrophic lakes and is able to maintain itself in both deep water and littoral environments, although it is only found above 50% abundance within the European database in lakes <20 m deep (Gasse et al., 1989; Cremer and Wagner, 2003). Valve preservation however is poor (**F** index ca. 0.3) and may be biased by differential preservation (Ryves et al., 2006; see Discussion).

Sedimentary pigments (12.5–225.0 nmol pigments g^{-1} OM) are also poorly preserved. There is a greater diversity of carotenoids as they are generally more stable than labile chlorophylls. β-carotene (most algae and plants; 0.6 nmol pigments g^{-1} OM) is a stable carotenoid, as is canthaxanthin (colonial cyanobacteria and herbivore tissues; 0.8 nmol pigments g^{-1} OM), indicating the core site may have experienced nutrient enrichment at this time. However, limited preservation precludes evaluation of phytoplankton community changes in this zone.

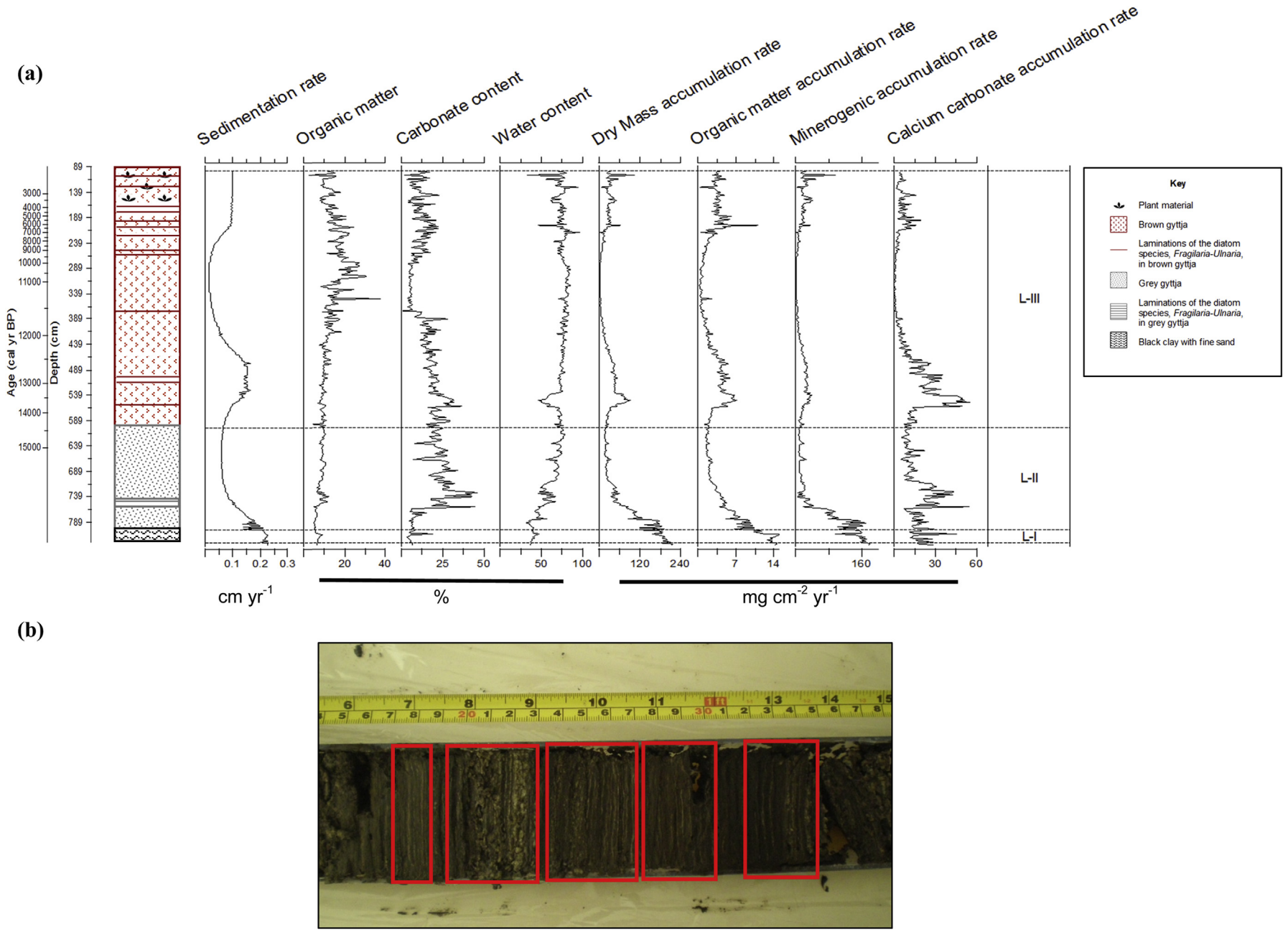

Fig. 3. (a) The three main lithostratigraphical units (L-I–III) identified in Hayk-01-2010. Organic, carbonate and water content are expressed as percentages of the total wet weight of the sediment, sedimentation accumulation rate as cm yr^{-1}, dry mass, organic matter, calcium carbonate ($CaCO_3$) and minerogenic accumulation rates as mg cm^{-2} yr^{-1}. (b) Photograph of a section of sediment from core 1B. The pulp-like dark yellow deposits identified are dense mats of the long, slender diatom taxa, *Fragilaria* and *Ulnaria*. (For interpretation of the references to colour in this figure legend, the reader is referred to the Web version of this article.)

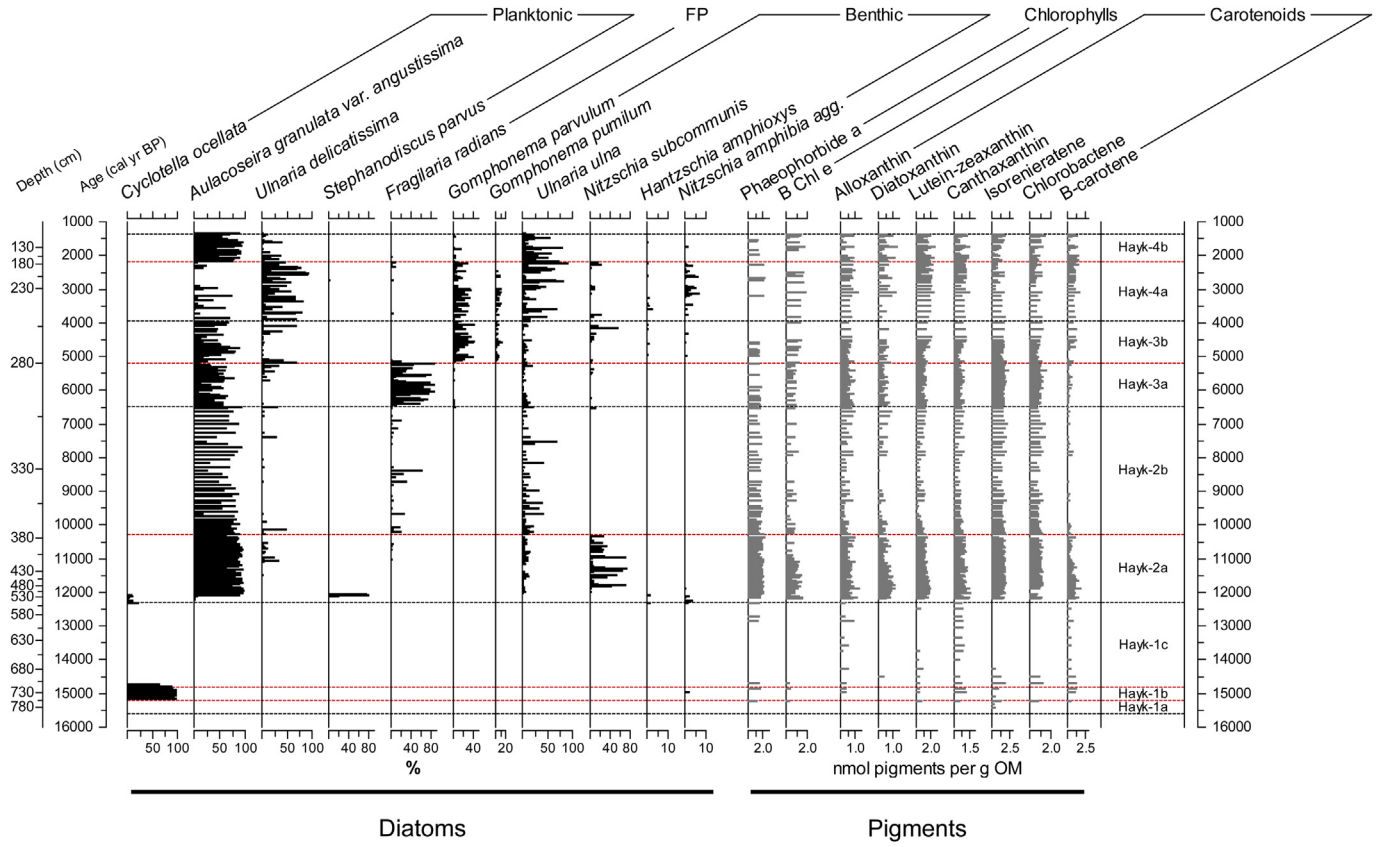

Fig. 4. Summary diagram of key diatom species and photosynthetic pigments. Diatom data are shown as a percentage (%) and pigments as concentration (nmol pigments g^{-1} OM).

4.2.3. Hayk-1c (716-553 cm, 14,800–12,300 cal yr BP)

The diatom record indicates an end to the wetter conditions at ca. 14,800 cal yr BP and a return to shallow lake conditions at the core site, evidenced by the decline and disappearance of *C. ocellata* (<5%). The intermittent presence of planktonic, facultatively planktonic and benthic taxa found in trace amounts suggests a fluctuating lake level; the core site may have been occasionally wet and fresh at times (however diatoms present are too few to permit any solid interpretation) but otherwise low, repeatedly drying out preventing the preservation of diatom taxa. Sedimentary pigments likewise indicate a poor preservation environment, based on the irregular pigment content. β-carotene (0.6 nmol pigments g^{-1} OM) and canthaxanthin (0.8 nmol pigments g^{-1} OM) are the only pigments to appear consistently throughout this zone, suggesting reduced productivity due to repeated desiccation of a shallow lake.

4.2.4. Hayk-2a (553-376 cm, 12,300–10,300 cal yr BP)

The transition from a shallow water body to a deeper, stable lake occurs at the start of this zone. The diatom assemblage is characterised by *C. ocellata* (24%) and *C. cyclopuncta* (18%), which are often found together today in moderately deep, oligotrophic to mesotrophic lakes in Europe (EDDI; Scussolini et al., 2011).

The periphytic and facultatively planktonic assemblage indicate that the lake level remained low, with the core site close to the littoral zone, while the presence of aerophilous forms such as *H. amphioxys* (2%) and littoral/subaerial *Nitzschia amphibia* (4%) may indicate sediment reworking from exposed margins of the basin (Chalié and Gasse, 2002b). Diatom-inferred conductivity confirms this variability in hydrology, with the lake interpreted as fresh with intermittent subsaline intervals (150–1000 μS cm^{-1}).

The increased diversity of sedimentary pigments (81.6 nmol pigments g^{-1} OM) indicates that preservation conditions at the core site improved. Diatoxanthin (siliceous algae; 1.0 nmol pigments g^{-1} OM), bacteriochlorophyll *e*, isorenieratene and chlorobactene (green sulphur bacteria; 1.6, 1.8 and 1.2 nmol pigments g^{-1} OM respectively) establish at this time. This indicates an availability of fresh, benthic conditions and occasional meromixis and bottom water anoxia, as documented in West Greenland lakes (McGowan et al., 2008).

Between approximately 12,100–12,050 cal yr BP a unique peak occurs in the record, characterised by the appearance of *Stephanodiscus parvus* (82%), which alternates in dominance with *Aulacoseira granulata* var. *angustissima* (27–91%). Within the constraints of dating, these seemingly multi-decadal fluctuations (ca.20–40 yrs) may suggest oscillations in nutrient availability (primarily the Si:P ratio) expressed as dominant decadal blooms, with high Si:P favouring *Aulacoseira* and low Si:P, *Stephanodiscus*. Both are planktonic taxa, indicating a deep, fresh (DI conductivity, ca. 90 μS cm^{-1}) lake and both can tolerate low light conditions (Kilham et al., 1986). Periods of *Aulacoseira* dominance suggest deeper mixing events bringing Si into the photic zone, while *Stephanodiscus* periods suggest stable stratification (reducing upwelling Si from depth).

A. granulata var. *angustissima* comes to dominate the diatom assemblage around 12,050 cal yr BP (82%), signalling moderately alkaline, eutrophic conditions (Kilham et al., 1986). Its increase in abundance in conjunction with the abrupt decline and disappearance of *S. parvus* indicates a greater availability of silicon in the lake, most likely a result of a major rise in lake depth and area, deeper mixing year-round and frequent upwelling of Si to the upper waters in response to a wetter climate.

A deep, stratified and productive lake system is in agreement

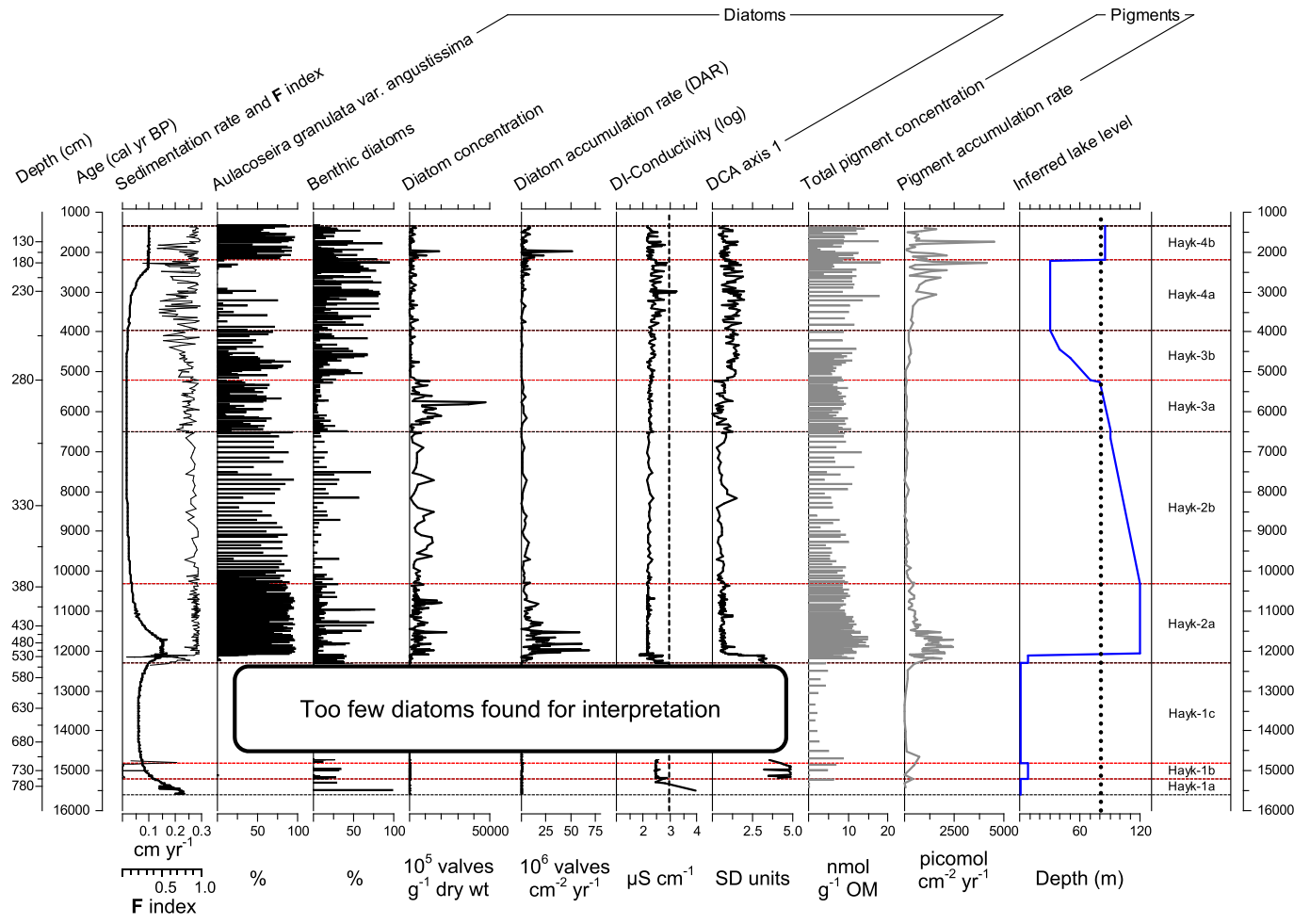

Fig. 5. Summary diagram of stratigraphic data from Lake Hayk. Sediment accumulation rate is expressed as cm yr^{-1} (thick line) overlain with diatom dissolution index (**F** index; thin line). Diatom data are shown as a percentage (%), concentration as x 10^5 g^{-1}, accumulation rate as x 10^6 valves cm^{-2} yr^{-1} and log diatom-inferred (DI) conductivity as µS cm^{-1}. Conductivity recorded in 1969 (920 µS cm^{-1}) is indicated by the red line (Baxter and Golobitsh, 1970). Total pigment concentration is shown as nmol pigments g^{-1} OM and accumulation rate as picomol cm^{-2} yr^{-1}. A simple lake level curve, representing maximum depth, is based on modern lake level data and interpretation of diatom and pigment proxies. Maximum lake level in 2000 (81.0 m; Lamb et al., 2007b) is indicated by the red line. (For interpretation of the references to colour in this figure legend, the reader is referred to the Web version of this article.)

with the sedimentary pigment record. High biological productivity is evidenced by the rapid increases in diatom and total pigment accumulation rates (67.9 × 10^6 valves cm^{-2} yr^{-1} and 2455 picomol cm^{-2} yr^{-1} respectively). The phytoplankton community is relatively stable in this zone with evidence of chlorophytes and cyanobacteria (lutein-zeaxanthin 2.3 nmol pigments g^{-1} OM), cryptophytes (alloxanthin 1.4 nmol pigments g^{-1} OM), siliceous algae (diatoxanthin 1.3 nmol pigments g^{-1} OM), which indicate the lake was most likely productive (McGowan, 2013). The high concentrations of pheophorbide *a* (2.5 nmol pigments g^{-1} OM) alongside low chlorophyll *a* concentrations (all algae and cyanobacteria, 0.8 nmol pigments g^{-1} OM), signal that zooplankton populations may have become established (Hurley and Armstrong, 1990). Green sulphur bacteria (bacteriochlorophyll *e*, isorenieratene and chlorobactene; 1.4, 2.1 and 1.7 nmol pigments g^{-1} OM respectively) indicate strong stratification and likely a chemocline, with long term anoxia in the hypolimnion (Hodgson et al., 1996). Excellent diatom preservation (**F** index = 0.99) with high sediment accumulation rates agrees with inferences of meromixis and deep water anoxia, reducing degradation of organic coatings on diatom frustules and enhancing silica preservation (Ryves et al., 2006).

Lake Hayk was most likely at its maximum extent and depth between 12.0 and 10.3 cal ka BP. The lake probably received overflow from Lake Hardibo at this time, assuming that Lake Hardibo was also at a highstand in response to the wetter, humid conditions. The overflow into Hayk would have caused its surface area to increase by up to three-fold (Ghinassi et al. 2012), allowing wind-driven mixing to dominate nutrient dynamics. Lake Hayk would have potentially overflowed into the Wazi River, creating a hydrologically open system, requiring the lake to have been ca. 40 m higher than present (Lamb et al., 2007b).

4.2.5. Hayk-2b (376-299 cm, 10,300–6500 cal yr BP)

Between 10.3 and 6.5 cal ka BP a gradual water level and lake area decline is inferred at Lake Hayk. *A. granulata* var. *angustissima* continues to dominate (96%) but abundance declines in conjunction with increases in facultatively planktonic and benthic taxa. The increase in *Ulnaria ulna* (71%) indicates availability of macrophytes in shallow benthic areas. Increases in the planktonic *Ulnaria delicatissima* (51%) and facultatively planktonic *Fragilaria radians* (63%) may also be indicative of lake level decline; Gasse (1986) identifies these varieties as important components of the plankton and bottom mud in small, shallow lakes, although it is also present in

deeper lakes. This assemblage indicates that water level was beginning to decline but the lake remained alkaline and fresh, confirmed by diatom-inferred conductivity (170 μS cm^{-1}).

Green sulphur bacteria continued to dominate the pigment record (bacteriochlorophyll *e*, isorenieratene and chlorobactene; 1.0, 2.4 and 1.6 nmol pigments g^{-1} OM respectively), indicating the lake remained deep enough to be meromictic. Cryptophytes, chrysophytes and dinoflagellates decline in this zone but total algal abundance remains relatively stable (9.5 nmol pigments g^{-1} OM), indicating productivity did not decline. Diatom (8.2×10^6 valves cm^{-2} yr^{-1}) and pigment (552 pmol cm^{-2} yr^{-1}) accumulation rate falls markedly from the previous zone. This marks a hydrological threshold when we suggest the lake essentially ceased to overflow into the Wazi River.

4.2.6. Hayk-3a (299-280 cm, 6500–5200 cal yr BP)

The diatom assemblage in Hayk-3a suggests the water level continued to fall, evidenced by further declines in *A.* var. *angustissima* (53%). Green sulphur bacteria indicate that Lake Hayk was still meromictic however, suggesting that lake depth had not declined to such an extent that the waterbody was completely mixed. The rapid increase in abundance of *F. radians* (83%) may indicate the point at which the permanent connection to Lake Hardibo was lost, resulting in lower lake level, reduced lake area and a relative decline in deeper mixing. The lake remained fresh (180 μS cm^{-1}), implying salts were effectively removed through groundwater outflow, and somewhat alkaline (Gasse, 1986).

Organic matter content remains high (ca. 20% OM), whilst accumulation rates for diatoms (5.5×10^6 valves cm^2 yr^{-1}), total pigments (115 picomol cm^{-2} yr^{-1}) and dry mass (2.8 mg cm^{-2} yr^{-1}) are low. While productivity was likely lower, this may be exaggerated by reduced sediment focussing at lower lake level as the basin filled with sediment. Diatom preservation remains good but shows a steady decline since the early Holocene, in keeping with inferences about increasing DI-conductivity and reducing lake level, both contributing to diatom dissolution.

4.2.7. Hayk-3b (280 - 257 cm, 5200–3950 cal yr BP)

A major water level decline is inferred at Lake Hayk between 5.20 and 3.95 cal ka BP, probably as a further depth threshold was crossed in response to continued long-term decline in effective moisture since the early Holocene. The littoral/benthic *Gomphonema parvulum* (20%) and *G. pumilum* (5%) increase in abundance, alongside an increase in the diversity of other periphytic taxa. This would suggest that as lake level declined, shallow near-shore sections of the lake basin were exposed and colonised, creating a greater availability of macrophyte habitat (Cocquyt, 1998). The lake was most likely shallower than its modern state (approximately 80–90 m maximum) and hydrologically closed (Umer et al., 2004; Lamb et al., 2007b).

Despite the decline in water level, Lake Hayk was still at least occasionally meromictic (potentially due to being shielded from deep wind mixing within its catchment), evidenced by the presence of green sulphur bacteria (isorenieratene and chlorobactene, 1.8 and 1.3 nmol pigments g^{-1} OM respectively), while pigments indicate populations of green algae, cryptophyte, dinoflagellate and chrysophytes. Diatom preservation declines marginally (**F** index of 0.8) while DI-conductivity rises persistently throughout the zone (200–300 μS cm^{-1}), which is consistent with hydrological closure.

4.2.8. Hayk-4a (257-173 cm, 3950–2200 cal yr BP)

The zone is largely dominated by *U. ulna* var. *ulna* (94%) and *U. delicatissima* (93%), although *Gomphonema* taxa remain important, as well as other benthic and facultatively planktonic taxa, indicating the proximity of the core site to the shore. The aerophilous *H. amphioxys* (4%) and *Nitzschia amphibia* var. *amphibia* (4%) increase in abundance, signalling sediment reworking and inwash from the catchment, or large scale colonisation of wetter margins, washing in littoral diatom valves.

The preservation of chlorophyll *a* (1.3 nmol pigments g^{-1} OM) indicates increased availability of phosphorus and a decrease in lake depth; potentially the diversity of benthic substrates would have encouraged growth of algae in the shallow regions of the lake, while also improving preservation by reducing sinking depth (McGowan, 2013). Fucoxanthin (siliceous algae; 1.8 nmol pigments g^{-1} OM) also indicates improved preservation as it is particularly labile (McGowan, 2013). Many chlorophyll degradation products are present however, indicative of mixing of the water column and an oxygenated photic sediment surface (Leavitt and Brown, 1988). Overall, the diatom and algal assemblage is typical of shallow, fresh-subsaline, mesotrophic-eutrophic eastern African lakes with an availability of epiphytic and epilithic habitats (Gasse, 1986).

Lake Hayk was at a Holocene lowstand, with DI conductivity reaching modern values on several occasions, with a maximum of 1800 μS cm^{-1} at ca. 3000 yr BP (230 cm), twice the modern value. Salt removal was less effective through reduced groundwater flows, allowing the lake to become subsaline at times. . Potentially Lake Hayk may have declined to 30 m or less, where the deeply shelving morphometry gives way to a larger, shallow expanse on the lake bottom, providing suitable habitat for benthic and periphytic algae.

4.2.9. Hayk-4b (173-89 cm, 2200–1350 cal yr BP)

A. granulata var. *angustissima* (97%) exhibits a rapid return to dominance, while the abundance and diversity of periphytic taxa generally decline, signifying a return to deep water with deep mixing. The disappearance of chlorophyll *a* also indicates an increase in lake depth (reducing preservation), which in conjunction with the re-establishment of green sulphur bacteria (bacteriochlorophyll *e*, isorenieratene and chlorobactene; 1.9, 2.1 and 1.6 nmol pigments g^{-1} OM respectively) implies the reoccurrence of meromixis and an anoxic hypolimnion. The rising sedimentation rate also points to a return to high lake level through enhanced sediment focussing, increasing diatom accumulation rates. DI conductivity indicates a return to freshwater conditions for much of the zone (ca.200 μS cm^{-1}), although values are on the cusp of being subsaline (670 μS $cm^{-}1$) in the early part, indicating a steady recovery rather than abrupt transition.

Lake depth may have been greatest at ca. 2 ka BP, when *A. granulata* var. *angustissima* dominates the diatom record, and diatom accumulation rate reaches levels not seen since the early Holocene. However, while there are strong similarities with conditions at the start of the Holocene, fluctuations in both diatom and pigment assemblages suggest rapid changes in limnological conditions and lake level. This is shown by major decreases in *A. granulata* var. *angustissima* in conjunction with increases in *U. ulna* var. *ulna* (82%) and *U. delicatissima* (4%). The phytoplankton assemblage is also indicative of short-term fluctuations in lake level as peaks in dinoflagellates, chrysophytes, euglenophytes and colonial cyanobacteria occur (diatoxanthin, lutein-zeaxanthin, canthaxanthin, 1,4, 2.8 and 1.5 nmol pigments g^{-1} OM respectively), synchronously with peaks in *Ulnaria ulna*.

5. Discussion: late Quaternary regional palaeohydrology and palaeoclimatology

The results are examined below in the context of other Ethiopian, eastern African and intertropical African palaeoenvironmental records from the late Pleistocene and Holocene, listed in Table 2 and displayed graphically in Figs. 6–8. When comparing records, consideration has been given to differences and

Table 2
Palaeo-records from Africa, the Mediterranean and Europe and their approximate termination of the African Humid Period.

Site	Country/Location	Map ID	Authority	Approximate AHP termination (cal kyr BP)
Lake Victoria	Rift Lake, 1°16′S	1	Stager et al. (1997)	7.2
Lake Albert	Rift Lake, 1°38′ N	2	Berke et al. (2014)	–
Lake Tanganyika	Rift Lake, 6°42′S	3	Tierney et al. (2010)	6.2
Lake Malawi	Rift Lake, 12°03′S	4	Konecky et al. (2011)	6.2
Lake Challa	Kenya, 3°19′S	5	Barker et al. (2013)	5.5
Lake Turkana	Kenya, 3°36′N	6	Morrissey and Scholz (2014)	5.2
Lake Tana	Ethiopia, 12°01′N	7	Marshall et al. (2011)	6.3
Lake Chad	Chad, 13°06′N	8	Armitage et al. (2015)	5
Lake Tritrivakely	Madagascar, 19°47′S	9	Gasse and Van Campo (1998)	4
Soreq cave	Israel, 31°45′N	10	Bar-Matthews and Ayalon (1997)	7
paleo- Lake Suguta	Kenya, 2°11′N	11	Junginger et al. (2013)	6.7
Chew Bahir	Ethiopia, 4°47′N	12	Foerster et al. (2012)	5
Ziway-Shala basin	Ethiopia, 7°58′N	13	Benvenuti et al. (2002)	5
Lake Hayk	Ethiopia, 11°20′N	14	This study	5.2
Lake Ashenge	Ethiopia, 12°34′N	15	Marshall et al. (2009)	5.6
Socotra Island	Yemen, 12°30′N	16	Shakun et al. (2007)	–
Gulf of Guinea	West Africa, 4°07′N	17	Armitage et al. (2015)	4.9
River Nile	Egypt, 30°49′N	18	Williams (2009)	4.3
Lake Naivasha	Kenya, 0°45′S	19	Bergner et al., 2003	–
Ebro desert	Spain,41°50′N	20	Davis and Stevenson (2007)	N/A
Lake Accesa	Italy, 42°59′N	21	Peyron et al. (2011)	N/A
Tenaghi Philippon	NE Greece	22	Peyron et al. (2011)	N/A
Antalaya	Turkey, 36°53′N	23	Weninger et al. (2006)	N/A
Gulf of Aden	Arabian Sea, 12°21′N	24	Tierney and deMenocal (2013)	5
Saqqara necropolis	Egypt, 29°51′N	25	Welc and Marks (2014)	5
Qunf cave	Oman, 17°10′N	26	Fleitmann et al. (2007)	7.8
Lake Yoa	Chad, 19°03′N	27	Kropelin et al. (2008)	5.6

discrepancies in dating methods and associated chronological accuracy and precision.

5.1. The late Pleistocene, 15.6–15.2 ka BP

The lowstand recorded at Lake Hayk at the start of the sequence ca. 15.6 ka BP reflects arid conditions throughout eastern and southern Africa and Asia associated with Heinrich Event 1 (HE-1; centred on 17–16 ka BP; Stager et al., 2011, Fig. 6). The collapse of the Afro-Asian Monsoon systems at this time and the regional weakening of the ITCZ have been linked to changes in Indian Ocean sea surface temperature (SST), through teleconnections from North Atlantic cooling following the iceberg rafting event of HE-1 (Denton et al., 2010). Arid events in other lakes and rivers across eastern and southern Africa and Asia, including the desiccation of the River Nile, at this time have been linked to HE-1; records from Lake Challa (Barker et al., 2013), Lake Bosumtwi (Peck et al., 2004), the Niger-Sanaga and Congo watersheds (Weijers et al., 2007; Weldeab et al., 2007) and northern Borneo (Partin et al., 2007) all indicate drying in response to HE-1.

The start of this arid phase at Hayk is not known as it precedes the base of the sequence at ca. 15.6 ka BP, but arid events recorded in other northern Ethiopian lake records are consistent with the timing of HE-1. At Lake Tana, Lamb et al. (2007a) using a simple hydrological model to reconstruct rainfall, estimated that precipitation was at most 40% of modern values. Lake Tana dried out sometime after 18.7 ka BP and remained closed until 15.7 ka BP when a *Cyperus* swamp developed at the centre of the lake basin (Marshall et al., 2011). Lake Ashenge may also have been exposed between 17.2 and 16.2 ka BP, evidenced by a relatively slow accumulation rate, compacted sediments and presence of aerophilous and other lake marginal diatom taxa (Marshall et al., 2009). The high rate of sediment accumulation inferred at Hayk at this time (Fig. 3[a]), despite ephemeral conditions, may be due to both greater minerogenic inputs from the catchment (e.g. fine sand; Fig. 3) and less certain dating control (with a wide dating envelope modelled in the base of the core; Fig. 2).

5.2. Start of the African Humid Period, 15.2–14.8 ka BP

An abrupt (ca. 100 years) shift towards wetter, more humid conditions at Lake Hayk is inferred at ca. 15.2 cal ka BP, evidenced by lithological changes and by the abundant pioneer freshwater diatom *C. ocellata* (Fig. 4). This transition coincides with the timing of rapid refilling at other tropical lake sites across Ethiopia and eastern Africa caused by increased monsoon strength at the onset of the AHP at ca. 15 ka BP (Figs. 6 and 7). The rejuvenation of the African-Indian monsoonal circulation has been attributed to the precessional increase in northern hemisphere summer insolation (Adkins et al., 2006). However, the onset of wetter conditions appears to vary in timing and rapidity among sites (Costa et al., 2014). This may reflect the varying behaviour of individual lake systems, as well as regional and topographic differences in air mass trajectories.

At Lake Ashenge an early return of wet conditions in the Ethiopian highlands is documented between ca. 16.2–15.2 ka BP, inferred from lake level rise following HE-1 (Marshall et al., 2009, Fig. 7[a]).). At Lake Tana, magnetic and geochemical data indicate abrupt lake deepening and flooding at 15.3–15.2 ka BP (Marshall et al., 2011; Loomis et al., 2015), causing the lake to overflow into the Blue Nile. This occurred at the same time as refilling at Lakes Victoria and Albert, the sources of the White Nile (Williams, 2009). As a result, flow in the main River Nile re-established between 14.7 and 14.5 ka BP (Williams, 2009; Box et al., 2011).

Elsewhere in eastern Africa, lake deepening at the onset of the AHP occurred in the Ziway-Shala basin (14.5 ka BP; Grove et al., 1975), Lake Turkana (14 ka BP; Morrissey and Scholz, 2014), Chew Bahir (14.5 ka BP; Foerster et al., 2012), palaeo-Lake Suguta (14.8 ka BP; Garcin et al., 2009) and at Lakes Magadi (Roberts et al., 1993), Manyara (Barker et al., 2004), Nakuru (Richardson and Dussinger, 1986), Challa (Tierney et al., 2011; Barker et al., 2013) and Tanganyika (Gasse et al., 1989; Costa et al., 2014) around 15 ka BP (Fig. 7 [a]). Refilling was not a rapid, linear process at all sites however, and some lakes such as Lakes Ashenge and Tanganyika show oscillations in lake level during this time.

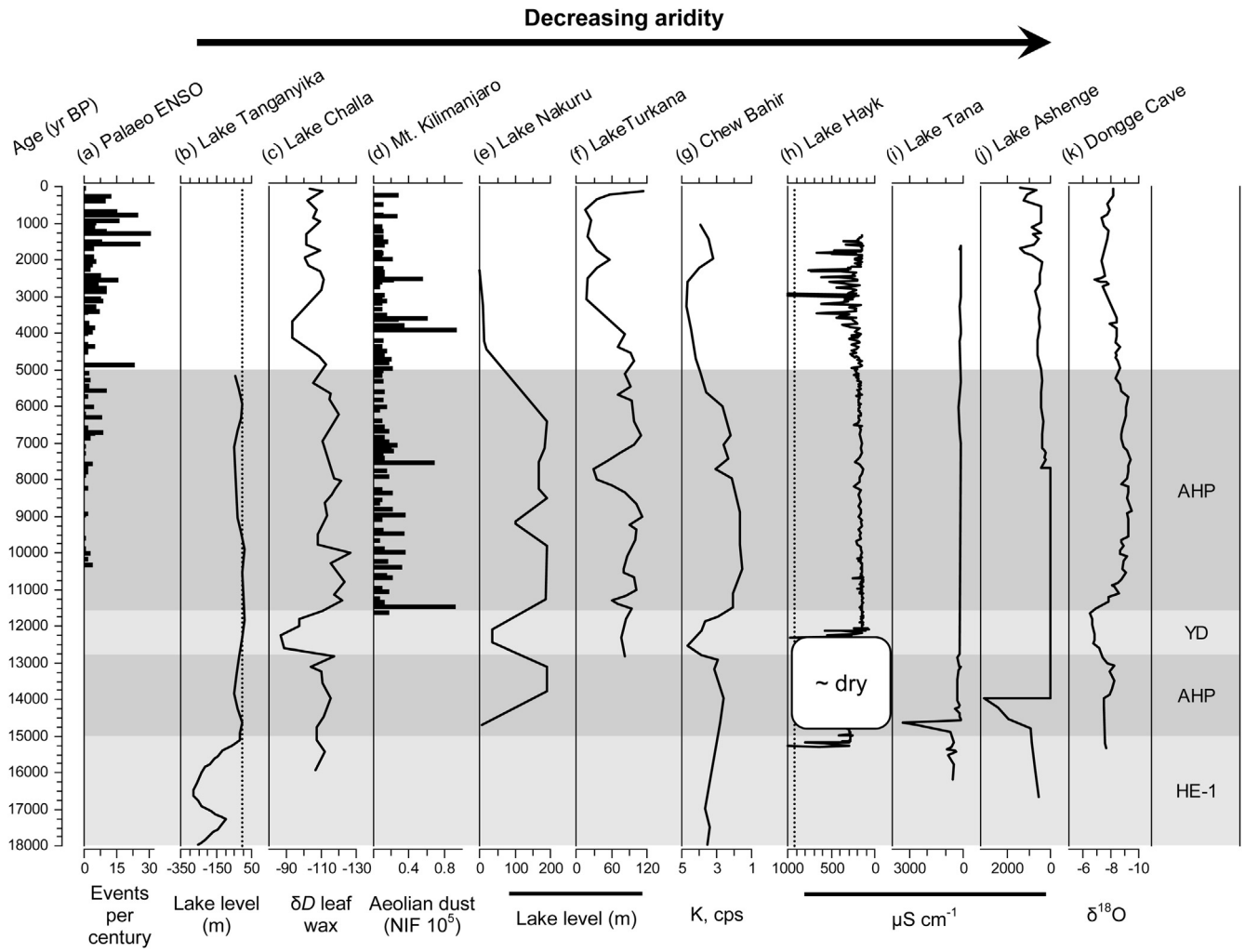

Fig. 6. Comparison of the onset and termination of eastern African lake levels and other palaeo-records, arranged in an *approximate* south to north order. Increasing lake level is to the right of all profiles. (**a**) Paleo-ENSO record from Laguna Pallcacocha, southern Ecuador (events per century; Moy et al., 2002). (**b**) Lake Tanganyika (height above present lake level; Gasse et al., 1989). (**c**) Lake Challa δ*D* leaf wax (Tierney et al., 2011); (**d**) Kilimanjaro aeolian dust record (NIF3 dust 10^5; Thompson et al., 2002); (**e**) Nakuru lake level (Richardson and Dussinger, 1986); (**f**) Turkana lake level (Brown and Fuller, 2008); (**g**) Chew Bahir potassium (K, cps) content (Foerster et al., 2012); (**h; this study**) Hayk diatom-inferred (DI) conductivity (μS cm^{-1}); (**i**) Tana DI conductivity (Marshall, 2006); (**j**) Ashenge DI conductivity (Marshall et al., 2009); (**k**) Dongge cave oxygen-isotope record (Dykoski et al., 2005). Key time periods identified are indicated: **HE-1**-Heinrich Event 1, **AHP**-African Humid Period and **YD**-Younger Dryas. Note the reversed axes for Lakes Challa, Chew Bahir, Hayk, Tana, Ashenge and the Dongge Cave record.

Discrepancies in the timing of the AHP onset, due to factors other than chronological uncertainty, probably reflect local manifestations of individual lake hydrology, variability in precipitation, water vapour transport and convection over eastern Africa caused by shifts in the position of major convergence zones such as the Congo Air Boundary. These air masses are in turn affected by SST variability in the Atlantic and Indian Oceans, the Red Sea and Mediterranean (Nicholson, 2000; Tierney et al., 2011). As such, Costa et al. (2014) propose a time-transgressive change in atmospheric circulation caused by a north-south migration of the tropical rain belts and an east-west migration of the Congo Air Boundary, as suggested at this site.

5.3. The deglacial transition, 14.8–12.3 ka BP: evidence of regional climatic heterogeneity

Lake Hayk dried and contained little water between ca. 14.8–12.3 cal ka BP (Figs. 4 and 6[h]). Lake Ashenge also experienced the onset of drying later, at ca. 13.6 ka BP, evidenced by maximum enriched $\delta^{18}O$ and $\delta^{13}C$ of authigenic carbonates and enhanced aragonite precipitation, signalling a highly negative water balance and lake shallowing (Marshall et al., 2009). This contrasts with most records from Ethiopian and eastern African lakes, which continued to refill to highstands following the beginning of the AHP (Fig. 7 [a,b]; Beuning et al., 1997; Gasse et al., 2002; Barker et al., 2004; Garcin et al., 2009; Foerster et al., 2012). These lakes then demonstrate a shift to aridity between 12.8 and 11.6 ka BP synchronous with high-latitude European Younger Dryas Stadial. The Younger Dryas proper does not appear at Lake Hayk at 12.8 cal yr BP; instead the lake refilled and deepened (Figs. 6 and 7). Potentially, the dry period documented at ca. 14.8–12.3 cal ka BP is the Younger Dryas with anomalous dating. Blaauw et al. (2011) estimate age offsets of between 200 and 450 years for dating of bulk organic carbon samples from Lake Challa. However, whilst dating errors may explain in part the age offsets identified in this record, the differences in the timing and length of the dry period beginning 14.8 cal ka BP are considerable and it seems unlikely to be caused purely by a dating issue.

Alternatively, Lake Hayk may show evidence of regional climatic heterogeneity, as documented in other Ethiopian and African sites

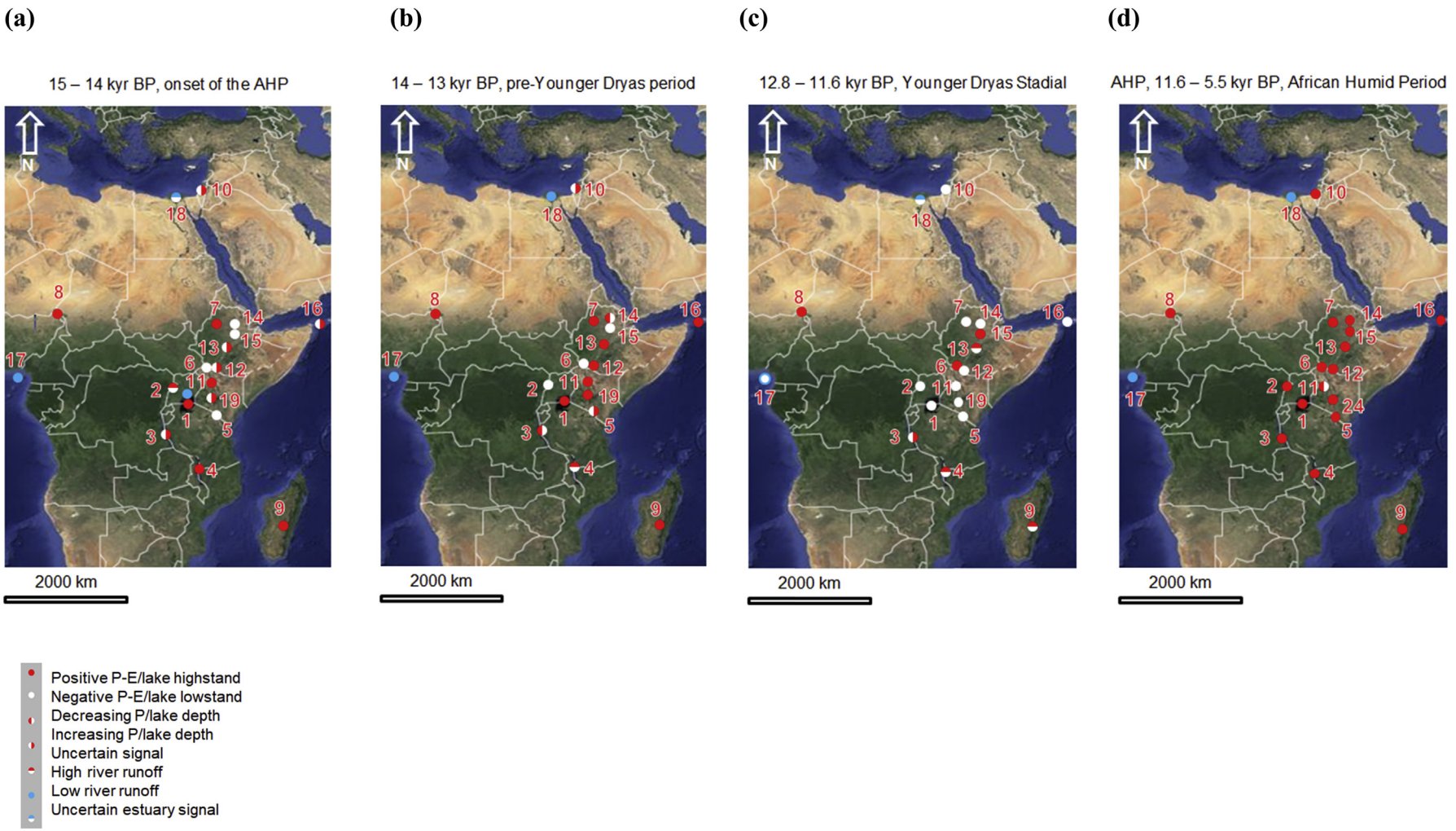

Fig. 7. Site map of records showing average hydrological conditions between (**a**) 15–14 ka BP; (**b**) the onset of the African Humid Period (AHP), 14–13 ka BP; (**c**) Younger Dryas Stadial, 12.8–11.6 ka BP; (**d**) The African Humid Period (AHP); 11.6–5.5 ka BP. Base map from Google Maps (2018). See Table 2 for references.

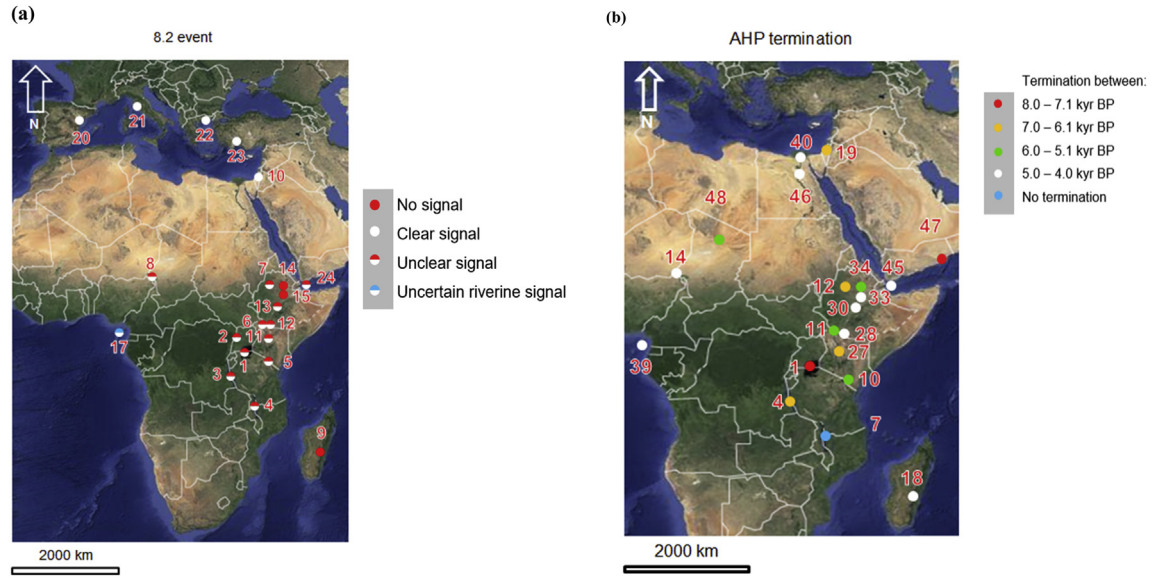

Fig. 8. Site map of records showing hydrological signal for (**a**) 8.2 ka BP and (**b**) African Humid Period (AHP) termination, 8.0–4.0 ka BP. Base map from Google Maps (2018). See Table 2 for references.

(Fig. 7[a, b]). At Lake Albert Berke et al. (2014) used the TEX_{86} temperature proxy, $\delta^{13}C_{wax}$ and δD analysis to reconstruct the climatic expression of the deglacial transition prior to the Younger Dryas. Between 13.8 and 11.5 ka BP, significant aridity and cooling (around 3 °C) occurred leading to a decline in lake level (Berke et al., 2014), reflecting Indian Ocean SST cooling, weakening the monsoon and reducing precipitation in this part of eastern Africa (see below). Cooling is similarly documented at Lakes Tanganyika (Tierney et al., 2008) and Malawi (Powers et al., 2005) between 13.8 and 13.6 ka BP, resulting in reduced lake levels. The cooling and drying documented prior to the Younger Dryas indicate a complex pattern of spatial and temporal change, coinciding with step-wise cooling in Greenland and the warm, wet Bølling-Allerød interstadial (ca. 14.7–12.8 ka BP) and the Antarctic Climatic Reversal cold interval (ACR, ca. 14.8–12.0 ka BP) (Alley and Clark, 1999). Beal et al. (2011) suggest that the ACR may have impacted the Agulhas Current by reducing the exchange of water between the Indian and Atlantic Oceans around Africa, subsequently weakening the Atlantic Meridional Overturning Circulation (AMOC). Reconstructions of the AMOC using $^{231}Pa/^{230}Th$, temperature proxies and $\delta^{13}C$ values of benthic foraminifera indicate reduced circulation strength at ca. 14 ka BP (Ritz et al., 2013). Although not as significant as at the Younger Dryas, this reduction may have been sufficient to cause anomalies in Indian Ocean SST and consequently weakened the Indian Ocean monsoon. This in turn triggering the cooling and drying observed at subtropical African lake sites as precipitation in the region decreased.

The aridity observed at Lake Hayk beginning ca. 14.7 cal ka BP (Figs. 4 and 6[h]) coincides with the proposed changes to the Indian Ocean monsoon system caused by the ACR and disturbance to the AMOC. It is likely that the drying reflects changes to the subtropical (northern and southern) monsoon alongside local, site-specific mechanisms affecting moisture delivery. This occurred during a period of complex climate change that remains poorly constrained in eastern African palaeo-records.

5.4. Resumption of the African Humid Period, 12.3–5.2 ka BP

While much of the rest of tropical Africa and the Arabian Peninsula remained dry until end of the Younger Dryas at ca. 11.6 ka BP, at Hayk permanent lake formation begins ca. 12.3 cal ka (Figs. 4, 6 and 7[c, d]). This signifies that the reactivation of the monsoon system across Africa and the Arabian Peninsula was first seen in central and northern Ethiopia (as the Ziway-Shala lakes also experience rising lake levels at this time; Benvenuti et al., 2002). Whilst there are uncertainties with dating methods, the earlier timing (ca. 700 years) of moisture increase at Hayk is beyond the likely error given the number of dates in this part of the sediment sequence, especially as such errors would be common to other records using bulk dates.

Regionally, other Ethiopian and eastern African lakes exhibit similar signals to Lake Hayk as highstands occurred between 13 and 5 ka BP in response to the resumption of the AHP (Figs. 6 and 7[c, d]; Bergner et al., 2003; Barker et al., 2004; Junginger et al., 2013). Lakes Tana, Tanganyika and Nakuru document highstands in the early Holocene (Fig. 6; Richardson and Dussinger, 1986; Gasse et al., 1989; Costa et al., 2014). At Lake Challa the most positive water balance occurred at ca. 11.5–9.8 ka BP, after which the lake level and aquatic productivity remained high (Tierney et al., 2011; Barker et al., 2013). Increasingly wet and humid conditions are also documented at sites in North Africa (Giraudi et al., 2012) and the Mediterranean (Bar-Matthews et al., 2000) at the start of the Holocene, including the formation of the eastern Mediterranean sapropels (Rohling and Hilgen, 1991).

There does not appear to be any significant change or variability in the palaeolimnological record at Lake Hayk in response to the drought event at ca. 8.2 ka BP. With improved dating an arid episode pertaining to the event may become identifiable and constrained, as there are subtle but distinct diatom assemblage changes at this time (Fig. 5). However, even if identified, it did not have such an extreme effect on the lake system as other arid events such as HE-1 or the Younger Dryas Stadial. Potentially, the drought may not be recorded because the event was not an abrupt occurrence caused by catastrophic melt water outburst, but was rather a fluctuation in a long-term background climatic anomaly (Rohling and Palike, 2005). Most subtropical African lakes do not exhibit a clear climatic response to the 8.2 ka BP event (Fig. 8[a]). Where a fluctuation is evident (several hundred years either side of 8.2 ka BP, within the margin of dating errors), it more likely reflects long-term changes in eastern African climate. For example, Marshall

et al. (2011) argues that the decline in rainfall at Lake Tana from ca. 8.5 ka BP onwards is due to the gradual migration of the tropical rain belts southward. This has also been identified by Stager et al. (2003) in a study of the White Nile and would account for the long-term decline in water level at Hayk from the early to mid-Holocene, rather than an abrupt shift centred at 8.2 ka BP.

5.5. Termination of the African Humid Period, 5.2–3.9 ka BP

The diatom and pigment records indicate Lake Hayk experienced a seemingly rapid termination of the African Humid Period, following a long-term decline in lake depth (Figs. 4, 5 and 8[b]). Between ca. 10.0–6.4 cal ka BP a gradual decline in lake depth is observed in the diatom data, but it is not until ca. 5.2 cal ka BP that major changes in the diatoms and phytoplankton are observed; a substantial increase in benthic diatom taxa occurs, signalling an increasingly arid climate.

It is tentatively interpreted therefore, that the AHP termination, in terms of diatom and pigment response, was relatively abrupt, spanning ca. 600 cal years between ca. 5.2–4.6 cal ka BP. This is broadly synchronous with regional records and closest to that of Lake Turkana, which is placed at 5270 ± 300 yr BP (Tierney and deMenocal, 2013) and Lake Edward, which is also placed at 5.2 ka BP (Ivory and Russell, 2018). This reflects the north to south diminishing strength of the summer monsoon, and progressively less northward penetration of the ITCZ (Shanahan et al., 2015).

However, despite this latitudinal decline in precipitation, lake responses to the termination do not mirror this north to south trend (Table 2; Fig. 8[b]). The earliest recorded responses are identified at Qunf cave, Oman (Fleitmann et al., 2007) and Lake Victoria (Stager et al., 1997) and the later signals from the River Nile (Williams, 2009), Lake Chad (Armitage et al., 2015), Lake Tritrivakely (Gasse and Van Campo, 1998) and the Gulf of Aden (Tierney and deMenocal, 2013). Therefore, there is no discernible geographic pattern in terms of climatic response to the termination of the AHP across Africa (Fig. 8[b]). This contrasts to the conclusion of Shanahan et al. (2015) of a time-transgressive termination which occurred later at lower latitudes as the rain-belts migrated southwards. The termination at Lake Hayk is neither significantly early nor late in comparison to other records from Ethiopia, the Horn of Africa or subtropical Africa, but in combination with these other records, emphasises the heterogeneous pattern of regional response to this climatic event across the African continent.

The theoretical duration of the AHP termination ranges from 280 to 490 years in the Gulf of Aden records and ~1000 years at Chew Bahir (Foerster et al., 2012). Palaeo-Lake Suguta similarly shows a gradual transition (Junginger and Trauth, 2013). The termination at Lake Hayk lasted around 600 years, making it neither exceptionally rapid nor long. The non-linear response of palaeorecords suggests the abruptness of the termination is caused by feedback mechanisms that enhance or suppress the transition. These mechanisms are not well understood but may be site-specific positive feedbacks caused by vegetation and soil moisture coupled with albedo, ocean temperature-moisture feedback, or differences in lake morphometry (Garcin et al., 2012; Junginger and Trauth, 2013). Clearly more research is needed on well-dated, high-resolution records form a suite of lakes and other sites in eastern Africa to address this uncertainty and provide high quality palaeodata for climate modelling hindcasts.

5.6. The late Holocene, 3.9–1.3 ka BP

Following the AHP termination a lowstand occurred at Hayk from ca. 3.9–2.2 cal ka BP (Figs. 4 and 6[h]). The lake became subsaline at times in response to a negative water balance. There is no evidence of the 4.2 arid event at Lake Hayk, despite suggestion by Ghinassi et al. (2012) that a lowstand identified in fluvial and coastal deposits in the Ankarka River area and stromatolitic deposits in Uarababo area of the lake were due to the event. This is more likely due to the lowstand beginning at ca. 3.9 cal ka BP, or the termination of the AHP.

Similarly to Lakes Ashenge, Turkana and Chew Bahir (Fig. 6), Lake Hayk saw an increase in lake depth and wetter conditions at ca. 2.2 cal ka BP, evidenced by the rise of planktonic diatoms in both records, and the surface connection to Lake Hardibo may have become re-established at times. This wet period lasted until at least ca. 1.3 cal ka BP, when the core Hayk-10 ends and is most likely the same highstand identified in the Uarababo and Ankarka River districts from 2.6 to 0.95 ka BP (Ghinassi et al., 2012). There is tentative evidence of a drop in water level at Hayk at ca. 1.5 cal ka BP. This may coincide with a similar shift observed at Lake Ashenge at 1.5 ka BP, signalling a move towards aridity (Marshall et al., 2009).

The relatively rapid shifts in aridity-humidity at Lake Hayk during the late Holocene may reflect higher frequency variability in the El Niño Southern Oscillation regime (ENSO) caused by cooling of the Pacific tropical deep waters (Foerster et al., 2012, Fig. 6[a, h]). In particular, a period of heightened ENSO activity centred from 2.5 to 1.6 cal ka BP (Fig. 6) may account for the variability seen in the upper Lake Hayk record, as ENSO events are linked to more recent increases in regional rainfall across eastern Africa (Nicholson, 2000). The Hayk-10 sequence ends at ca. 1.3 cal ka, although sedimentation continues to the present day (Lamb et al., 2007b).

6. Conclusion

The palaeolimnological records obtained from Lake Hayk using a multi-proxy approach have successfully provided high-resolution evidence of millennial to multi-decadal variability in the lake. Changes identified since ca. 15.6 cal ka BP includes variability in productivity and trophic state, stratification and overturn, catchment weathering and erosion, preservation, lake level and conductivity.

At the millennial scale, the palaeolimnological records indicate that local climate at Hayk has been sensitive to high-latitude glacial conditions, which have been paced by variations in insolation, and changes in Earth's orbital precession. Hayk experienced the same transitions from arid to humid and humid to arid as experienced by other lake sites across eastern Africa since the Last Glacial Maximum, including high-magnitude events such as HE-1 (ca. 18.0–15.0 ka BP), the onset and termination of the African Humid Period (ca. 15.0–5.0 ka BP) and the Younger Dryas Stadial (ca. 12.8–11.6 ka BP).

Though broadly synchronous, there are discrepancies in the precise timing and expression of climatic events and comparison of Lake Hayk sedimentary record to other sites from the region shows variability in the nature of climate shifts. Minor discrepancies may be attributed to chronological uncertainties and have been identified where possible. Beyond this, response to climatic change reflects the inherent climatic sensitivity of individual lake basin characteristics. Such differences are the likely cause of discrepancies between the Hayk, Tana and Ashenge records, despite their proximity to one another, as well as discrepancies between Hayk and other sites across Ethiopia and eastern Africa. Given such local, site-specific factors, synthesising records from across a landscape is vital for identifying the full nature of regional Quaternary climate change. The Lake Hayk palaeo-record therefore has an important role to play in bridging knowledge gaps in the currently under-represented, data-sparse and climatically vulnerable north of Ethiopia.

Acknowledgements

With thanks to the the University of Cologne CRC (Collaborative Research Centre) 806 for funding core collection: http://www.sfb806.uni-koeln.de/index.php/projects/former-projects/a3. Thanks to Oliver Langkamp (student co-worker at Cologne University) for his help preparing and performing the coring. Three AMS 14C dates were awarded to Katie Loakes under the the QRA-14CHRONO Centre Radiocarbon Dating award, supported by supported by Prof Paula Reimer (14CHRONO centre, Queens University Belfast). Katie Loakes was supported by a Loughborough University PhD award. Keely Mills publishes with the approval of the Executive Director, British Geological Survey (NERC). We thank both reviewers for their thoughtful and constructive comments which have helped improve the manuscript.

Appendix A. Supplementary data

Supplementary data to this article can be found online at https://doi.org/10.1016/j.quascirev.2018.09.005.

References

Adkins, J., deMenocal, P., Eshel, G., 2006. The "African humid period" and the record of marine upwelling from excess ^{230}Th in Ocean Drilling Program Hole 658C. Paleoceanography 21, 1–14. https://doi.org/10.1029/2005PA001200. PA4203.

Alley, R.B., Clark, P.U., 1999. The deglaciation of the Northern Hemisphere: a global perspective. AREPS 27, 149–182.

Armitage, S.C., Bristow, C.S., Drake, N.A., 2015. West African monsoon dynamics inferred from abrupt fluctuations of Lake Mega-Chad. Proc. Natl. Acad. Sci. Unit. States Am. 112, 8543–8548.

Barker, P.A., Hurrell, E.R., Leng, M.J., Plessen, B., Wolff, C., Conley, D.J., Keppens, E., Milne, I., Cumming, B.F., Laird, K.R., Kendrick, C.P., Wynn, P.M., Verschuren, D., 2013. Carbon cycling within an East African lake revealed by the carbon isotope composition of diatom silica: a 25-ka record from Lake Challa, Mt. Kilimanjaro. Quat. Sci. Rev. 66, 55–63.

Barker, P.A., Talbot, M.R., Street-Perrott, F.A., Marret, F., Scourse, J., Odada, E.O., 2004. Late Quaternary climatic variability in intertropical Africa. In: Battarbee, R.W., Gasse, F., Stickley, C.E. (Eds.), Past Climate Variability through Europe and Africa. Springer, Dordrecht, pp. 117–138.

Bar-Matthews, M., Ayalon, A., 1997. Late Quaternary paleoclimate in the Eastern Mediterranean region from stable isotope analysis of speleothems at Soreq Cave, Israel. Quat. Res. 47, 155–168.

Bar-Matthews, M., Ayalon, A., Kaufman, A., 2000. Timing and hydrological conditions of Sapropel events in the Eastern Mediterranean, as evident from speleothems, Soreq cave, Israel. Chem. Geol. 169, 145–156.

Baxter, R.M., Golobitsch, D.L., 1970. A note on the limnology of Lake Hayk, Ethiopia. Limnol. Oceanogr. 15, 144–148.

Beal, L.M., De Ruijter, W.P.M., Biastoch, A., Zahn, R., 2011. On the role of the Agulhas system in ocean circulation and climate. Nature 472, 429–436.

Bennett, K.D., 1995-2007. Psimpoll and Pscomb Programs for Plotting and Analysis. Available at: http://www.chrono.qub.ac.uk/psimpoll/psimpoll.html.

Bennett, K.D., 1996. Determination of the number of zones in a biostratigraphical sequence. New Phytol. 132, 155–170.

Benvenuti, M., Carnicelli, S., Belluomini, G., Dainelli, N., Di Grazia, S., Ferrari, G.A., Iasio, C., Sagri, M., Ventra, D., Atnafu, B., Kebede, S., 2002. The Ziway-Shala lake basin (main Ethiopian rift, Ethiopia): a revision of basin evolution with special reference to the Late Quaternary. J. Afr. Earth Sci. 35, 247–269.

Beuning, K.R.M., Talbot, M., Kelts, K., 1997. A revised 30,000-year palaeoclimatic and palaeohydrologic history of Lake Albert, East Africa. Palaeogeogr. Palaeoclimatol. Palaeoecol. 136, 259–279.

Bergner, A.G.N., Trauth, M.H., Bookhagen, B., 2003. Paleoprecipitation estimates for the Lake Naivasha basin (Kenya) during the last 175 k.y. using a lake-balance model. Global Planet. Lett. 36, 117–136.

Berke, M.A., Johnson, T.C., Werne, J.P., Livingstone, D., Grice, K., Schouten, S., Sinninghe Damsté, J.S., 2014. Characterization of the last deglacial transition in tropical East Africa: insights from lake Albert. Palaeogeogr. Palaeoclimatol. Palaeoecol. 409, 1–8.

Blaauw, M., 2010. Methods and code for 'classical' age-modelling of radiocarbon sequences. Quat. Geochronol. 5, 512–518.

Blaauw, M., van Geel, B., Kristen, I., Plessen, B., Lyaruu, A., Engstrom, D.R., van der Plicht, J., Verschuren, D., 2011. High-resolution 14C dating of a 25,000-year lake-sediment record from equatorial East Africa. Quat. Sci. Rev. 30, 3043–3059.

Box, M.R., Krom, M.D., Cliff, R.A., Bar-Matthews, M., Almogi-Labin, A., Ayalon, A., Paterne, M., 2011. Response of the Nile and its catchment to millennial-scale climate change since the LGM from Sr isotopes and major elements of East Mediterranean sediments. Quat. Sci. Rev. 30, 431–442.

Brown, E.T., Fuller, C.H., 2008. Stratigraphy and tephra of the Kibish formation, southwestern Ethiopia. J. Hum. Evol. 55, 366–403.

Chalié, F., Gasse, F., 2002a. A 13,500 year diatom record from the tropical East African Rift Lake abiyata (Ethiopia). Palaeogeogr. Palaeoclimatol. Palaeoecol. 187, 259–284.

Chalié, F., Gasse, F., 2002b. Late Glacial-Holocene diatom record of water chemistry and lake level change from the tropical East African Rift Lake Abiyata (Ethiopia). Palaeogeogr. Palaeoclimatol. Palaeoecol. 187, 259–283.

Chen, N., Bianchi, T.S., McKee, B.A., Bland, J.M., 2001. Historical trends of hypoxia on the Louisiana shelf: application of pigments as biomarkers. Org. Geochem. 32, 543–561.

Cocquyt, C., Vyverman, W., Compere, P., 1993. A check-list of the algal flora of the east african great lakes (Malawi, Tanganyika and Victoria). Meise: National Botanic Garden of Belgium.

Cocquyt, C., 1998. Diatoms from the northern basin of lake Tanganyika. In: Bibliotecha Diatomologica Band, vol. 39. J. Cramer in der Gebrüder Borntraeger Verlagsbuchhandlung, Berlin.

Costa, K., Russell, J., Konecky, B., Lamb, H.F., 2014. Isotopic reconstruction of the african Humid Period and Congo air boundary migration At lake Tana, Ethiopia. Quat. Sci. Rev. 83, 58–67.

Cremer, H., Wagner, B., 2003. The diatom flora in the ultra-oligotrophic Lake El'gygytgyn, Chukotka. Polar Biol. 26, 105–114.

Darbyshire, I., Lamb, H.F., Umer, M., 2003. Forest clearance and regrowth in northern Ethiopia during the last 3000 years. Holocene 13, 537–546.

Davis, B.A.S., Stevenson, A.C., 2007. The 8.2 ka event and Early–Mid Holocene forests, fires and flooding in the Central Ebro Desert, NE Spain. Quat. Sci. Rev. 13–14, 1695–1712.

Dean, W., 1974. Determination of carbonate and organic matter in calcareous sediments and sedimentary rocks by loss on ignition: comparison with other methods. J. Sediment. Petrol. 44, 242–248.

Demelie, M., Ayenew, T., Wohnlich, S., 2007. Comprehensive hydrological and hydrogeological study of topographically closed lakes in highland Ethiopia: The case of Hayq and Ardibo. J. Hydrol. 339, 145–158.

Denton, G.H., Anderson, R.F., Toggweiler, J.R., Edwards, R.L., Schaefer, J.M., Putnam, A.E., 2010. The last glacial termination. Science 328, 1652–1656.

Dykoski, C.A., Edwards, R.L., Cheng, H., Yuan, D., Cai, Y., Zhang, M., Lin, Y., Qing, J., An, Z., Revenaugh, J., 2005. A high-resolution, absolute dated Holocene and deglacial Asian monsoon record from Dongge Cave, China. Earth Planet Sci. Lett. 233, 71–86.

Fleitmann, D., Burns, S.J., Mangini, A., Mudelsee, M., Kramers, J., Villa, I., Neff, U., Al-Subbary, A.A., Buettner, A., Hippler, D., Matter, A., 2007. Holocene ITCZ and Indian monsoon dynamic recorded in stalagmites from Oman and Yemen (Socotra). Quat. Sci. Rev. 26, 170–188.

Foerster, V., Junginger, A., Langkamp, O., Gebru, T., Asrat, A., Umer, M., Lamb, F.H., Wennrich, V., Rethemeyer, J., Nowaczyk, N., Trauth, M.H., Schaebtz, F., 2012. Climatic change recorded in the sediments of the Chew Bahir basin, southern Ethiopia, during the last 45,000 years. Quat. Int. 274, 25–37.

Garcin, Y., Junginger, A., Melnick, D., Olago, D.O., Strecker, M.R., Trauth, M.H., 2009. Late pleistocene-holocene rise and collapse of lake Suguta, northern Kenya rift. Quat. Sci. Rev. 28, 911–925.

Garcin, Y., Melnick, D., Strecker, M.R., Olago, D.O., Tiercelin, J.J., 2012. East African mid-Holocene wet-dry transition recorded in palaeo-shorelines of Lake Turkana, northern Kenya Rift. Earth Planet Sci. Lett. 331–332, 322–334.

Gasse, F., 1986. East African diatoms; Taxonomy, ecological distribution. In: Bibliotheca Diatomologica, vol. 11. J. Cramer in der Gebrüder Borntraeger Verlagsbuchhandlung, Berlin.

Gasse, F., Barker, P., Johnson, T.C., 2002. A 24,000 yr diatom record from the northern basin of Lake Malawi. In: Odada, E.O., Olago, D.O. (Eds.), The East-African Great Lakes: Limnology, Palaeolimnology and Biodiversity. Kluwer Academic Publishers, The Netherlands, pp. 393–414.

Gasse, F., Lédée, V., Massault, M., Fontes, J.C., 1989. Water-level fluctuations of Lake Tanganyika in phase with oceanic changes during the last glaciation and deglaciation. Nature 342, 57–59.

Gasse, F., Van Campo, E., 1998. A 40,000-yr pollen and diatom record from Lake Tritrivakely, Madagascar, the southern tropics. Quat. Res. 49, 299–311.

Ghinassi, M., D'Oriano, F., Benvenuti, M., Awramik, S., Bartolini, C., Fedi, M., Ferrari, G., Papini, M., Sagri, M., Talbot, M., 2012. Shoreline fluctuations of Lake Hayk (northern Ethiopia) during the last 3500 years: geomorphological, sedimentary and isotope records. Palaeogeogr. Palaeoclimatol. Palaeoecol. 365–366, 209–226.

Giraudi, C., Mercuri, A.M., Esu, D., 2012. Holocene palaeoclimate in the northern Sahara margin (Jefara Plain, northwest Libya). Holocene 23, 339–353.

Google Maps, 2018. Continental Africa. Available at: https://www.google.co.uk/maps/@3.9519411,26.3671879, 11485228m/data=!3m1!1e 3?hl=en. (Accessed 23 September 2018).

Grove, A.T., Street, F.A., Goudie, A.S., 1975. Former lake levels and climatic change in the Rift Valley of southern Ethiopia. Geogr. J. 141, 177–194.

Hammer, U.T., 1986. Saline Lake Ecosystems of the World (Monographiae Biologicae). Dr. W. Junk Publishers, Dordrecht.

Hodgson, D.A., Tyler, P., Vyvermanm, W., 1996. The palaeolimnology of Lake Fidler, a meromictic lake in south-west Tasmania and the significance of recent human impact. J. Paleolimnol. 18, 313–333.

Hurley, J.P., Armstrong, D.E., 1990. Fluxes and transformations of aquatic pigments in Lake Mendota, Wisconsin. Limnol. Oceanogr. 35, 384–398.

Hustedt, F., 1949. Süßwasser-Diatomeen aus dem Albert-National park in Belgisch–Kongo. Exploratie van het National Albert.

Ivory, S.J., Russell, J., 2018. Lowland forest collapse and early human impacts at the end of the African Humid period at Lake Edward, equatorial East Africa. Quat. Res. 89, 7–20.
Johnson, T.C., 1996. Sedimentary processes and signals of past climatic change in the large lakes of the East African Rift Valley. In: Johnson, T.C., Odada, E.O. (Eds.), The Limnology, Climatology and Paleoclimatology of the East African Lakes. Gordon and Breach Publishers, The Netherlands, pp. 367–412.
Juggins, S., 2007. In: C2 Version 1.5 User Guide. Software for Ecological and Palaeoecological Data Analysis and Visualisation. Newcastle University, Newcastle upon Tyne, UK, p. 73.
Junginger, A., Roller, S., Olaka, L.A., Trauth, M.H., 2013. The effects of solar irradiation changes on the migration of the Congo Air Boundary and water levels of paleo-Lake Suguta, Northern Kenya Rift, during the African Humid Period (15–5 ka BP). Palaeogeogr. Palaeoclimatol. Palaeoecol. 396, 1–16.
Junginger, A., Trauth, M.H., 2013. Hydrological constraints of paleo-Lake Suguta in the northern Kenya rift during the african Humid Period (15– 5 ka BP). Global Planet. Sci. 111, 174–188.
Kilham, P., Kilham, S.S., Hecky, R.E., 1986. Hypothesized resource relationships among African planktonic diatoms. Limnol. Oceanogr. 31, 1169–1181.
Konecky, B.L., Russell, J.M., Johnson, T.C., Brown, E.T., Berke, M.A., Werne, J.P., Huang, Y., 2011. Atmospheric circulation patterns during the late Pleistocene climate changes at Lake Malawi, Africa. Earth Planet Sci. Lett. 312, 318–326.
Krammer, K., Lange-Bertalot, H., 1988. In: Süßwasserflora von Mitteleuropa, 2/2 Bacillariophyceae, 2. Teil: Bacillariaceae, Epithemiaceae, Surirellaceae. Gustav Fischer Verlag, New York, p. 596.
Krammer, K., Lange-Bertalot, H., 1991a. In: Süßwasserflora von Mitteleuropa, 2/3 Bacillariophyceae, 3. Teil: Centrales, Fragilariaceae, Eunotiaceae. Gustav Fischer Verlag, Berlin, p. 576.
Krammer, K., Lange-Bertalot, H., 1991b. In: Süßwasserflora von Mitteleuropa, 2/4 Bacillariophyceae, 4. Teil: Achnanthaceae Kritische Ergansungen zu Achnanthes s.l, Navicula s.str., Gomphonema. Gustav Fischer Verlag, Berlin, p. 437.
Krammer, K., Lange-Bertalot, H., 1999. In: Süßwasserflora von Mitteleuropa, 2/1 Bacillariophyceae, 1. Teil: Naviculaceae. Gustav Fischer Verlag, New York, p. 876.
Kropelin, S., Verschuren, D., Lezine, A.M., Eggermont, H., Cocquyt, C., Francus, P., Cazet, J.P., Fagot, M., Rumes, B., Russell, J.M., Darius, F., Conley, D.J., Schuster, M., von Suchodoletz, H., Engstrom, D.R., 2008. Climate-driven ecosystem succession in the Sahara: the past 6000 years. Science 320, 765–768.
Lamb, H.F., Bates, C.R., Coombes, P.V., Marshall, M.H., Umer, M., Davies, S.J., Dejen, E., 2007a. Late Pleistocene desiccation of lake Tana, source of the blue nile. Quat. Sci. Rev. 26, 287–299.
Lamb, H.F., Leng, M.J., Telford, R.J., Ayenew, T., Umer, M., 2007b. Oxygen and carbon isotope composition of authigenic carbonate from an Ethiopian lake: a climate record of the last 2000 years. Holocene 17, 515–524.
Leavitt, P.R., Brown, S.R., 1988. Effects of grazing by *Daphnia* on algal carotenoids: implications for paleolimnology. J. Paleolimnol. 1, 201–213.
Loakes, K., 2015. Late Quaternary Palaeolimnology and Environmental Change in the South Wollo Highlands, Ethiopia. PhD thesis. Loughborough University.
Loomis, S.E., Russell, J.M., Lamb, H.F., 2015. Northeast african temperature variability since the late Pleistocene. Palaeogeogr. Palaeoclimatol. Palaeoecol. 423, 80–90.
Marshall, M.H., 2006. Late Pleistocene and Holocene Palaeolimnology of Lakes Tana and Ashenge, Northern Ethiopia. PhD thesis. University of Wales.
Marshall, M.H., Lamb, H.F., Davies, S.J., Leng, M.J., Kubsa, Z., Umer, M., Bryant, C., 2009. Climatic change in northern Ethiopia during the past 17,000 years: a diatom and stable isotope record from Lake Ashenge. Palaeogeogr. Palaeoclimatol. Palaeoecol. 279, 114–127.
Marshall, M.H., Lamb, H.F., Huws, D., Davies, S.J., Bates, R., Bloemendal, J., Boyle, J., Leng, M.J., Umer, M., Bryant, C., 2011. Late Pleistocene and Holocene drought events At lake Tana, source of the blue nile. Global Planet. Change 78, 147–161.
McGowan, S., 2013. Pigment studies. In: Elias, S.A. (Ed.), The Encyclopedia of Quaternary Science, vol. 3. Elsevier, Amsterdam, pp. 326–338.
McGowan, S., Juhler, R.K., Anderson, N.J., 2008. Autotrophic response to lake age, conductivity and temperature in two West Greenland lakes. J. Paleolimnol. 39, 301–317.
Morrissey, A., Scholz, C.A., 2014. Paleohydrology of lake Turkana and its influence on the nile river system. Palaeogeogr. Palaeoclimatol. Palaeoecol. 403, 88–100.
Moy, C.M., Seltzer, G.O., Rodbell, D.T., Anderson, D.M., 2002. Variability of El niño/southern oscillation activity at millennial timescales during the Holocene epoch. Nature 420, 162–165.
Nicholson, S.E., 2000. The nature of rainfall variability over Africa on time scales of decades to millennia. Global Planet. Change 26, 137–158.
Patrick, R., Reimer, C.W., 1966. In: The Diatoms of the United States Exclusive of Alaska and Hawaii, vol. 1. Monographs of the Academy of Natural Sciences of Philadelphia, USA, p. 13.
Partin, J.W., Cobb, K.M., Adkins, J.F., Clark, B., Fernandez, D.P., 2007. Millennial-scale trends in west Pacific warm pool hydrology since the Last Glacial Maximum. Nature 449, 452–455.
Peck, J.A., Green, R.R., Shanahan, T., King, J.W., Overpeck, J.T., Scholz, C.A., 2004. A magnetic mineral record of Late Quaternary tropical climate variability from Lake Bosumtwi, Ghana. Palaeogeogr. Palaeoclimatol. Palaeoecol. 215, 37–57.
Peyron, O., Goring, S., Dormoy, I., Kotthoff, U., Pross, J., de Beaulieu, J.L., Drescher-Schneider, R., Vannière, B., Magny, M., 2011. Holocene seasonality changes in the central Mediterranean region reconstructed from the pollen sequences of Lake Accesa (Italy) and Tenaghi Philippon (Greece). Holocene 21, 131–146.
Powers, L.A., Johnson, T.C., Werne, J.P., Castaneda, I.S., Hopmans, E.C., Sinninghe Damsté, J.S., Schouten, S., 2005. Large temperature variability in the southern african tropics since the last glacial maximum. Geophys. Res. Lett. 32, 1–4.
Richardson, J.L., Dussinger, R.A., 1986. Paleolimnology of mid-elevation lakes in the Kenya rift valley. Hydrobiologia 143, 167–174.
Ritz, S.P., Stocker, T.F., Grimalt, J.O., Menviel, L., Timmermann, A., 2013. Estimated strength of the Atlantic overturning circulation during the last deglaciation. Nat. Geosci. 6, 208–212.
Roberts, N., Taieb, M., Barker, P., Damnati, B., Icole, M., Williamson, D., 1993. Timing of the younger Dryas event in east Africa from Lake-level changes. Nature 366, 146–148.
Rohling, E.J., Hilgen, F.J., 1991. The eastern Mediterranean climate at times of sapropel formation: a review. Geol. Mijnbouw 70, 253–264.
Rohling, E.J., Palike, H., 2005. Centennial-scale climate cooling with a sudden cold event around 8,200 years ago. Nature 434, 975–979.
Roy, S., Llewellyn, C.A., Egeland, E.S., Johnsen, G. (Eds.), 2011. Phytoplankton Pigments Characterization, Chemotaxonomy and Applications in Oceanography. Cambridge University Press, Cambridge.
Ryves, D.B., Battarbee, R.W., Juggins, S., Fritz, S.C., Anderson, N.J., 2006. Physical and chemical predictors of diatom dissolution in freshwater and saline lake sediments in North America and West Greenland. Limnol. Oceanogr. 51, 1355–1368.
Schnurrenberger, D., Russell, J., Kelts, K., 2003. Classification of lacustrine sediments based on sedimentary components. J. Paleolimnol. 29, 141–154.
Scussolini, P., Vegas-Vilarrúbia, T., Rull, V., Corella, J.P., Valero-Garcés, B., Gomà, J., 2011. Middle and late Holocene climate change and human impact inferred from diatoms, algae and aquatic macrophyte pollen in sediments from Lake Montcortès (NE Iberian Peninsula). J. Paleolimnol. 46, 369–385.
Shakun, J.D., Burns, S.J., Fleitmann, D., Kramers, J., Matter, A., Al-Subary, A., 2007. A high-resolution, absolute-dated deglacial speleothem record of Indian Ocean climate from Socotra Island, Yemen. Earth Planet Sci. Lett. 259, 442–456.
Shanahan, T.M., McKay, N.P., Hughen, K.A., Overpeck, J.T., Otto-Bliesner, B., Heil, C.W., King, J., Scholz, C.A., Peck, J., 2015. The time-transgressive termination of the african Humid Period. Nat. Geosci. 8, 140–144.
Stager, J.C., Cumming, B.F., Meeker, L.D., 1997. A high-resolution 11 400-yr diatom record from lake Victoria, East Africa. Quat. Res. 47, 81–89.
Stager, J.C., Cumming, B.F., Meeker, L.D., 2003. A 10,000-year high-resolution diatom record from Pilkington Bay, Lake Victoria, East Africa. Quat. Res. 59, 172–181.
Stager, J.C., Ryves, D.B., Chase, B.M., Pausata, F.S.R., 2011. Catastrophic drought in the afro-asian monsoon region during Heinrich event 1. Science 331, 1299–1302.
Stuiver, M., Reimer, P.J., 1993. Extended 14C database and revised CALIB radiocarbon calibration program. Radiocarbon 35, 215–230.
Tierney, J.E., deMenocal, P.B., 2013. Abrupt shifts in Horn of Africa hydroclimate since the last glacial maximum. Science 342, 843–846.
Tierney, J.E., Russell, J.M., Huang, Y., 2010. A molecular perspective on Late Quaternary climate and vegetation change in the Lake Tanganyika basin, East Africa. Quat. Sci. Rev. 29, 787–800.
Tierney, J.E., Russell, J.M., Huang, Y., Sinninghe Damsté, J.S., Hopmans, E.C., Cohen, A.S., 2008. Northern Hemisphere controls on tropical southeast African climate during the past 60,000 years. Science 322, 252–255.
Tierney, J.E., Russell, J.M., Sinninghe Damsté, J.S., Huang, Y., Verschuren, D., 2011. Late quaternary behaviour of the east african monsoon and the importance of the Congo air boundary. Quat. Sci. Rev. 30, 798–807.
Thompson, L.G., Mosley-Thompson, E., Davis, M.E., Henderson, K.A., Brecher, H.H., Zagorodnov, V.S., Mashiotta, T.A., Lin, P.N., Mikhalenko, V.N., Hardy, D.R., Beer, J., 2002. Kilimanjaro ice core records: Evidence of Holocene climate change in tropical Africa. Science 298, 589–593.
Umer, M., Legesse, D., Gasse, F., Bonnefille, R., Lamb, H.F., Leng, M.L., Lamb, A.L., 2004. Late quaternary climate changes in the Horn of Africa. In: Battarbee, R.W., Gasse, F., Stickley, C.E. (Eds.), Past Climate Variability through Europe and Africa. Springer, The Netherlands, pp. 159–180.
Weijers, J.W.H., Schefuß, E., Schouten, S., Sinninghe Damsté, J.S., 2007. Coupled thermal and hydrological evolution of tropical Africa over the last deglaciation. Science 315, 1701–1704.
Welc, F., Marks, L., 2014. Climate change at the end of the Old Kingdom in Egypt around 4200 BP: New geoarchaeological evidence. Quat. Int. 324, 124–133.
Weldeab, S., Lea, D.W., Schneider, R.R., Andersen, N., 2007. 155,000 years of West African monsoon and ocean thermal evolution. Science 316, 1303–1307.
Weninger, B., Alram-Stern, E., Bauer, E., Clare, L., Danzeglocke, U., Jöris, O., Kubatzki, C., Rollefson, G., Todorova, H., van Andel, T., 2006. Climate forcing due to the 8200 cal yr BP event observed at Early Neolithic sites in the eastern Mediterranean. Quat. Res. 66, 401–420.
Williams, W.D., 1967. The chemical characteristics of lentic surface waters in Australia: a review. In: Weatherley, A.H. (Ed.), Australian Inland Waters and Their Fauna. Australia National University Press, Canberra, pp. 18–77.
Williams, M.A.J., 2009. Late Pleistocene and Holocene environments in the nile basin. Global Planet. Change 69, 1–15.
Yesuf, H.M., Alamirew, T., Melesse, A.M., Assen, M., 2013. Bathymetric study of lake Hayk, Ethiopia. Lakes Reservoirs Res. Manag. 18, 155–165.